First-principles calculation of the magnetocrystalline anisotropy energy of iron, cobalt, and nickel

G. H. O. Daalderop, P. J. Kelly, and M. F. H. Schuurmans
Philips Research Laboratories, P.O. Box 80 000, NL-5600 JA Eindhoven, The Netherlands
(Received 17 January 1990; revised manuscript received 13 April 1990)

The magnetocrystalline anisotropy energies of the elements iron, cobalt, and nickel have been calculated by means of the linear muffin-tin orbital (LMTO) method in the atomic-sphere approximation (ASA) within the framework of the local-spin-density approximation (LSDA). The so-called "force theorem" is used to express the total-energy difference, when spin-orbit coupling is included, as a difference in sums of Kohn-Sham single-particle eigenvalues. The results depend strongly on the location and dispersion of degenerate energy bands near the Fermi surface, and particular attention must be paid to the convergence of the Brillouin-zone integral of the single-particle eigenvalues. The calculated values of the anisotropy energy are too small by comparison with experiment, and we do not predict the correct easy axis for cobalt and nickel. We find that the variation of the anisotropy energy with changes in strain, in the magnitude of the spin-orbit coupling, for different choices of the exchange-correlation potential and for varying numbers of valence electrons are not capable of explaining these incorrect results. By comparing our calculated energy bands with those obtained by a full-potential linear augmented plane wave (FLAPW) method we conclude that the discrepancy is not attributable to terms in the potential that are neglected in the ASA.

I. INTRODUCTION

A long-standing problem which has recently received much attention is that of describing the magnetocrystalline anisotropy energy (MAE) of magnetic materials containing transition-metal elements. Thin layers of iron on copper are found to have their magnetic moments oriented perpendicular to the plane of the monolayer.[1] In our own laboratory it has been found that in Pd/Co superlattices a switch of the easy (-magnetization) axis from in plane to out of plane occurs as a function of the Co thickness.[2] A detailed understanding of the mechanisms responsible for these phenomena is still lacking. It would be very useful if theory could offer some guidelines as to what determines the anisotropy of a particular material. At the same time it should be realized that the MAE of even iron, cobalt, and nickel is not well understood, partly because it is so small. At low temperatures ($T=4.2$ K) it is of the order of 60 μeV/atom for (uniaxial) hcp cobalt[3] and for cubic iron and nickel it is a factor of 50 smaller.[4] It is the purpose of this paper to investigate the possibility of calculating magnetocrystalline anisotropy energies from first principles. Because of the large number of experimental and theoretical studies of Fe, Co, and Ni we choose them as a test for our method.

The theory of MAE in the 3*d* transition metals has a long history. In the earliest attempts to understand the MAE of iron, cobalt, and nickel the magnetic moments were considered to be localized on the atoms comprising the solid. As described by van Vleck,[5] the MAE is electrostatic in origin, the mutual electrostatic energy between two atoms depending on the orientation of the localized spin and orbital moments relative to one another and relative to the axis joining them. The corresponding Hamiltonian is replaced by a spin Hamiltonian incorporating a molecular field term as well as dipole-dipole and quadrupole-quadrupole coupling terms which are electrostatic in origin. The coupling constants are then larger than if they were due to purely magnetostatic forces. The anisotropy energy is found by the application of perturbation theory.

Brooks,[6] and later Fletcher,[7] used an itinerant-electron model to explain the MAE and the quenching of orbital angular momentum in cubic crystals. A broadening of crystal-field-split states smaller than the crystal-field separation was assumed to occur for the *d* electrons. Treating the spin-orbit coupling as a perturbation, fourth-order perturbation theory was used to obtain the cubic anisotropy. Most subsequent work has been concerned with extending this model. One line of investigation has concentrated on explaining the MAE of Fe, Co, and Ni by using more realistic band structures than those originally employed by Brooks and Fletcher.[8–13] A second line of investigation has been to examine the effect of symmetry reduction on the anisotropy energy. Most of this work, which was concerned with the possibility of finding large MAE's at the surfaces of magnetic transition-metal elements, was of a qualitative nature.[14]

More recently attempts have been made to calculate MAE's from first principles for bulk crystalline Fe, Co, and Ni (Refs. 15–17) as well as for Ni and Fe films.[18–20] Because the MAE is a ground-state property it can, at least in principle, be determined within Hohenberg-Kohn density-functional theory[21] in which the many-electron problem is reduced to an effective independent-particle problem.[22–26] Although the local-spin-density approximation (LSDA) (Ref. 27) to the exchange-correlation energy has been remarkably successful in describing many ground-state properties of solids, there have been some

 ©1990 The American Physical Society

exceptions,[23,24] particularly in relation to the ferromagnetic 3*d* transition-metal elements. The incorrect structure found for the ground state of Fe (Ref. 28) indicates errors in total-energy differences which are of the order of tens of meV's. Within the simplifying framework of the LSDA it is still not a trivial matter to compute energy differences which are only of the order of μeV. All calculations of the MAE which we are aware of approximate the total-energy difference as the difference in the sums of single-particle eigenvalues occurring in the Kohn-Sham equations. No attempt has been made to establish the realm of validity of this approximation.

In the case of a free-standing monolayer of (001) Fe, the anisotropy energy has been calculated to be of the order of 1 meV and because the Brillouin-zone integration must only be performed in two dimensions it is possible to study the convergence of the integral with respect to the number of sampling points. However Gay and Richter[18] predict the easy axis to be perpendicular to the plane of the monolayer and find an anisotropy energy of -0.4 meV/atom whereas Karas *et al.* calculate a value of 3.4 meV/atom with the easy direction of magnetization lying in the plane of the monolayer.[19] Both LSDA calculations appear to be adequately converged. A direct comparison with experiment is not possible because it is believed that the interaction of the magnetic monolayer with the substrate can change the value of the anisotropy energy substantially.[20] In the case of Fe and Ni where the anisotropy energy is experimentally well known,[3,4] it is still not clear what the final LSDA prediction is and there are substantial discrepancies between the values which have been reported.[15–17] This is related to the difficulty of calculating the very small energy differences involved sufficiently reliably.

Some of these issues will be addressed in this publication. Because we are interested in understanding the experimental results for metallic superlattices,[2] where little or nothing is known about the underlying electronic structure, we have chosen to use an *ab initio* method. It will be necessary to diagonalize a Hamiltonian at a large number of **k** vectors ($\sim$500 000 for Ni), so it is important to use an efficient method to solve the band-structure problem. We have chosen to use the linear muffin-tin orbital (LMTO) method in the atomic-sphere approximation (ASA).[29,30] We will see that our calculations raise considerable doubt as to the possibility of calculating the MAE correctly on a scale of <100 μeV using the approximations made at present. Before attributing the failure to the LSDA, an attempt must be made to improve upon the approximation of the total-energy difference as a difference of single-particle eigenvalue sums.

The paper is organized as follows. In Sec. II the method used to calculate the MAE and the nature of the approximations made are discussed. In Sec. III we present numerical results relating to the issue of the convergence of the single-particle eigenvalue sum for iron, cobalt, and nickel. We compare these results with experiment in Sec. IV and consider several possible explanations for the disagreement. In Sec. V we discuss previous calculations in light of our findings, and finally in Sec. VI we draw some conclusions.

II. METHOD

In this section the various approximations we make in order to calculate the MAE will be outlined. Because the spin-orbit interaction responsible for the magnetocrystalline anisotropy is small compared to the exchange-splitting and the band dispersion, we will adopt the simplified but transparent procedure of treating it as a perturbation with respect to those other effects.[29,31,32] In Sec. II A we describe this in more detail. This approach has the advantage that the problem of calculating the difference in total energy for two directions of magnetization may be approximated as the difference of two single-particle eigenvalue sums (Sec. II B). Whether one makes these approximations or not, an integral of the eigenvalues over the occupied part of the Brillouin zone must be performed with μeV precision. Technical aspects of the Brillouin-zone integration are discussed in Sec. II C. In order to solve the band-structure problem we use the LMTO-ASA method. Some of the approximations inherent in this method which are relevant to the calculation of the MAE are discussed in Sec. II D. Finally we discuss in Sec. II E the magnetostatic contribution to the MAE of iron, cobalt, and nickel.

A. Form of the Hamiltonian

For the 3*d* electrons in Fe, Co, and Ni, the spin-orbit coupling parameter ξ_d is $\sim$70 meV. The mass-velocity and Darwin shifts, which are also relativistic effects of order v^2/c^2 (where c is the velocity of light and v a typical conduction-electron velocity), give rise to a shift of the 4*s* band relative to the 3*d* band of the order of 150 meV. By comparison, the 3*d* bandwidth is $\sim$4 eV and the exchange splitting is approximately $mI_{\rm xc}$, where m is the magnetic moment per atom and $I_{\rm xc}$, the Stoner parameter, is $\sim$1 eV for Fe, Co, and Ni.[33,34]

The spin-orbit interaction and the mass-velocity and Darwin shifts are taken into account most simply by solving the two-component Pauli equation

$$(\mathcal{H}^{\rm SR}+\mathcal{H}^{\rm SO})\Psi(\mathbf{r})=\varepsilon\Psi(\mathbf{r}) , \tag{1}$$

where the Hamiltonian has been split into a spin-polarized scalar-relativistic part which will be treated fully self-consistently and the spin-orbit interaction which will be added in the last iteration of the self-consistent field procedure. In the atomic-sphere approximation, the potential is taken to have spherical symmetry inside atomic spheres which replace the atomic Wigner-Seitz cell. Inside an atomic sphere $\mathcal{H}^{\rm SR}$ has a particularly simple form:[35]

$$\mathcal{H}^{\rm SR}_{\alpha\beta}=\left[-\nabla^2+v(r)-\frac{1}{c^2}\left[(\varepsilon-v(r))^2+\frac{\partial v(r)}{\partial r}\frac{\partial}{\partial r}\right]\right]\delta_{\alpha\beta} + \left[\frac{\delta E_{\rm xc}}{\delta\rho_{\alpha\beta}(\mathbf{r})}-\frac{\delta E_{\rm xc}}{\delta\rho(\mathbf{r})}\delta_{\alpha\beta}\right] , \tag{2}$$

where $v(\mathbf{r})$ is given by

$$v(\mathbf{r})=v_{\rm ext}(\mathbf{r})+2\int d\mathbf{r}'\frac{\rho(\mathbf{r}')}{|\mathbf{r}-\mathbf{r}'|}+\frac{\delta E_{\rm xc}}{\delta\rho(\mathbf{r})} \tag{3}$$

and Rydberg atomic units are used. $v_{\rm ext}$ is the external (ionic) potential and the electron density $\rho(\mathbf{r})=\mathrm{Tr}\underline{\rho}(\mathbf{r})$, where $\underline{\rho}(\mathbf{r})$ is the density matrix with components $\rho_{\alpha\beta}(\mathbf{r})=\sum_{i,\mathbf{k}}^{\rm occ}[\Psi_\beta^{i,\mathbf{k}}(\mathbf{r})]^*\Psi_\alpha^{i,\mathbf{k}}(\mathbf{r})$. The summation is over all occupied bands, $\varepsilon_i(\mathbf{k})<\varepsilon_F$, where i is the band index and $\mathbf{k}$ is the Bloch vector [omitted for simplicity in (2)]. The trace is taken over the spin indices. For a homogeneous spin-polarized electron gas with only two nonzero components of the spin density, $\rho_\uparrow$ and $\rho_\downarrow$, the exchange-correlation energy per particle is $\varepsilon_{\rm xc}(\rho_\uparrow,\rho_\downarrow)$. In the local-spin-density approximation (LSDA) (Refs. 22 and 27) the exchange-correlation energy for an inhomogeneous electron gas, $E_{\rm xc}$, is approximated by

$$E_{\rm xc}[\rho_\uparrow,\rho_\downarrow]=\int d\mathbf{r}\,\rho(\mathbf{r})\varepsilon_{\rm xc}(\rho_\uparrow,\rho_\downarrow)\ . \tag{4}$$

The eigenstates of $\mathcal{H}^{\rm SR}$ have pure spin character so that in the absence of spin-orbit coupling the last two terms in (2) may be written as $\mathbf{b}(\mathbf{r})\cdot\sigma$ in terms of the exchange field,

$$\mathbf{b}(\mathbf{r})=\hat{\mathbf{n}}\frac{\delta E_{\rm xc}}{\delta m(\mathbf{r})}\ , \tag{5}$$

where $\hat{\mathbf{n}}$ is an arbitrarily chosen magnetization direction. The electron density $\rho(\mathbf{r})=\rho_\uparrow(\mathbf{r})+\rho_\downarrow(\mathbf{r})$ and the spin density $m(\mathbf{r})=\rho_\uparrow(\mathbf{r})-\rho_\downarrow(\mathbf{r})$. When the spin-orbit interaction

$$\mathcal{H}^{\rm SO}=\tfrac{1}{2}\xi(r)\boldsymbol{l}\cdot\underline{\boldsymbol{\sigma}}=c^{-2}\frac{1}{r}\frac{\partial v(r)}{\partial r}\begin{bmatrix} l_z & l_- \\ l_+ & -l_z\end{bmatrix}\ , \tag{6}$$

coupling the spin-up and spin-down equations is included, the density matrix $\underline{\rho}(\mathbf{r})$ is in general nondiagonal. The electron density is then $\rho(\mathbf{r})=\mathrm{Tr}\underline{\rho}(\mathbf{r})$ and the spin density $\mathbf{m}(\mathbf{r})=\mathrm{Tr}\{\underline{\boldsymbol{\sigma}}\underline{\rho}(\mathbf{r})\}$.

There is some ambiguity about whether or not the potential used to calculate the mass-velocity and Darwin shifts and the spin-orbit coupling parameter should include the contribution from the exchange field. However, in practice the consequences of doing this are negligible and we use the average of the spin-up and spin-down potentials, as indicated in Eqs. (2) and (6). Other relativistic terms of order v^2/c^2 or higher have been shown to give rise to negligible changes in the electronic energy bands.[36,35] The formal incorporation of relativistic effects into density-functional theory has been discussed in Ref. 25 and reviewed in Ref. 26.

B. Total-energy calculation

Magnetocrystalline anisotropy energies are of the order of 1 μeV/atom for iron and nickel, and approximately 60 μeV/atom for cobalt. This should be compared with the total energy per atom which is of the order of 40 000 eV/atom. Assuming that the contribution of the core states to the anisotropy energy is negligible and making the frozen-core approximation,[37] the total conduction electron energy is of the order of 500 eV and the anisotropy energy is only $\sim 10^{-9}$ of this amount. We shall not attempt to calculate the total energy with this accuracy. Instead, we take advantage of the variational character of the total energy to express the change in total energy upon rotation of the magnetization direction as the difference in two sums of single-particle energies. Such a single-particle eigenvalue sum is of order 10 eV and we shall find that a calculation to 1 μeV precision is just feasible.

In our treatment of MAE, we start from a self-consistent spin-polarized scalar-relativistic calculation where the input density matrix to the last iteration is denoted $\underline{\rho}^o$. Because it has been constructed from eigenstates with pure spin character there is a single $\mathbf{r}$-independent transformation which diagonalizes $\underline{\rho}^o(\mathbf{r})$ with eigenvalues $\rho_\uparrow(\mathbf{r})$ and $\rho_\downarrow(\mathbf{r})$. A variational expression for the total energy is

$$E[\underline{\rho}^o,\underline{\rho}^n]=T[\underline{\rho}^o,\underline{\rho}^n]+U_H[\underline{\rho}^n]+E_{\rm xc}[\underline{\rho}^n]+E_{\rm ext}[\underline{\rho}^n]\ . \tag{7}$$

T, U_H, $E_{\rm xc}$, and $E_{\rm ext}$ are, respectively, the kinetic energy, electron-electron Coulomb interaction energy, exchange-correlation energy, and the sum of the electron-ion and ion-ion Coulomb interaction energies. The density matrix obtained on output from the last iteration (after applying $\mathcal{H}^{\rm SR}$) is denoted $\underline{\rho}^n$. Specifically,

$$\begin{aligned}T[\underline{\rho}^0,\underline{\rho}^n]=&\sum_{i,\mathbf{k}}^{\rm occ}\varepsilon_i(\mathbf{k})-2\int d\mathbf{r}\int d\mathbf{r}'\,\frac{\rho^o(\mathbf{r})\rho^n(\mathbf{r}')}{|\mathbf{r}-\mathbf{r}'|}\\&-\mathrm{Tr}\left[\int d\mathbf{r}\,\underline{\rho}^n(\mathbf{r})\underline{v}_{\rm xc}[\underline{\rho}^o(\mathbf{r})]\right]\\&-\int d\mathbf{r}\,\rho^n(\mathbf{r})v_{\rm ext}(\mathbf{r})\ ,\end{aligned} \tag{8}$$

where

$$v_{\rm xc}^{\alpha\beta}(\mathbf{r})=\frac{\delta E_{\rm xc}[\underline{\rho}(\mathbf{r})]}{\delta\rho_{\alpha\beta}(\mathbf{r})}\ , \tag{9}$$

$$U_H[\rho]=\int d\mathbf{r}\int d\mathbf{r}'\,\frac{\rho(\mathbf{r})\rho(\mathbf{r}')}{|\mathbf{r}-\mathbf{r}'|}\ , \tag{10}$$

and

$$E_{\rm ext}[\rho]=\int d\mathbf{r}\,\rho(\mathbf{r})v_{\rm ext}(\mathbf{r})+E_{\text{ion-ion}}\ . \tag{11}$$

In case of complete self-consistency $\underline{\rho}^o=\underline{\rho}^n$, but this is only ever approximately true in practice.

On adding $\mathcal{H}^{\rm SO}$ to $\mathcal{H}^{\rm SR}$, and solving the corresponding Kohn-Sham equations (1) *non-self-consistently*, the slightly different total energy $E(\hat{\mathbf{n}})$, energy eigenvalues $\varepsilon_i(\hat{\mathbf{n}},\mathbf{k})$, and density matrix $\underline{\rho}'^n$ are obtained. Because the spin-orbit interaction is small compared to the bandwidth and the exchange splitting, we expect the change in the total energy to be small. It can be expressed as

$$\Delta E(\hat{\mathbf{n}}) = E(\hat{\mathbf{n}}) - E$$
$$= \sum_{i,\mathbf{k}}^{\text{occ}} \varepsilon_i(\hat{\mathbf{n}},\mathbf{k}) - \sum_{i,\mathbf{k}}^{\text{occ}} \varepsilon_i(\mathbf{k}) - 2\int d\mathbf{r}\int d\mathbf{r}' \frac{\rho^o(\mathbf{r})\delta\rho^n(\mathbf{r}')}{|\mathbf{r}-\mathbf{r}'|} + 2\int d\mathbf{r}\int d\mathbf{r}' \frac{\rho^n(\mathbf{r}')\delta\rho^n(\mathbf{r})}{|\mathbf{r}-\mathbf{r}'|}$$
$$- \mathrm{Tr}\left[\int d\mathbf{r}\, \underline{v}_{\mathrm{xc}}[\underline{\rho}^o]\delta\underline{\rho}^n(\mathbf{r})\right] + E_{\mathrm{xc}}(\underline{\rho}^n+\delta\underline{\rho}^n) - E_{\mathrm{xc}}[\underline{\rho}^n] + O[(\delta\underline{\rho}^n)^2] , \tag{12}$$

where $\delta\underline{\rho}^n = \underline{\rho}'^n - \underline{\rho}^n$. Omitting terms of order $(\delta\underline{\rho}^n)^2$ and rearranging yields

$$\Delta E(\hat{\mathbf{n}}) = \sum_{i,\mathbf{k}}^{\text{occ}} \varepsilon_i(\hat{\mathbf{n}},\mathbf{k}) - \sum_{i,\mathbf{k}}^{\text{occ}} \varepsilon_i(\mathbf{k}) + 2\int d\mathbf{r}\int d\mathbf{r}' \frac{\Delta\rho(\mathbf{r}')\delta\rho^n(\mathbf{r})}{|\mathbf{r}-\mathbf{r}'|} + \mathrm{Tr}\left[\int d\mathbf{r}\, \Delta\underline{v}_{\mathrm{xc}}(\mathbf{r})\delta\underline{\rho}^n(\mathbf{r})\right] . \tag{13}$$

We have defined

$$\Delta\rho = \mathrm{Tr}(\underline{\rho}^n - \underline{\rho}^o)$$

and

$$\Delta\underline{v}_{\mathrm{xc}} = \underline{v}_{\mathrm{xc}}[\underline{\rho}^n] - \underline{v}_{\mathrm{xc}}[\underline{\rho}^o] .$$

We will now assume that the self-consistent calculation with $\mathcal{H}^{\mathrm{SR}}$ was so close to self-consistency that the last two terms in (13) involving $\Delta\rho$ and $\Delta\underline{v}_{\mathrm{xc}}$ may be neglected. However, this condition has not been fulfilled in all other first-principles calculations of the MAE and we will return to this point in Sec. V A.

Due to the variational character of the expression for the total energy, (7), the change in total energy is in first order in $\delta\rho^n$ given by the change in the sum over the occupied single-particle energies:

$$\Delta E(\hat{\mathbf{n}}) = \sum_{i,\mathbf{k}}^{\text{occ}} \varepsilon_i(\hat{\mathbf{n}},\mathbf{k}) - \sum_{i,\mathbf{k}}^{\text{occ}} \varepsilon_i(\mathbf{k}) . \tag{14}$$

This relation has been called the force theorem[38] and provides a formal justification for using single-particle eigenvalue sums to obtain total-energy differences. We note that in order for the total energy to be variational, the full density-matrix $\underline{\rho}^n$, and $\underline{\rho}'^n$, including nonspherical and nondiagonal terms, should, in principle, be used. To be able to use the standard local-density forms for $E_{\mathrm{xc}}[\rho_\uparrow,\rho_\downarrow]$ in this case, the spin density would have to be determined at every point $\mathbf{r}$ by diagonalizing the density matrix $\underline{\rho}^n(\mathbf{r})$. Subtraction of two total energies, determined from two self-consistent calculations, but using spherically symmetric charge densities or diagonal density matrices in the total-energy calculation, will not necessarily yield a more accurate answer than the force theorem.

How well does ΔE approximate the change in total energy on including spin-orbit coupling which would be obtained by solving (1) exactly? The calculated change in the sum of the single-particle energies is 9 meV/atom for nickel, 8 meV/atom for cobalt, and 6 meV/atom for iron. A self-consistent calculation is expected to differ from this amount by a factor of order $\sim\xi\langle \underline{l}\cdot\underline{\sigma}\rangle/2mI_{\mathrm{xc}}$. Taking $\xi=70$ meV, $\langle l\rangle=0.1$, $\langle m\rangle=\langle\underline{\sigma}\rangle$, and $I_{\mathrm{xc}}=950$ meV, we expect the first-order approximation to be accurate to about a half percent. A calculation where $\mathcal{H}$, including the spin-orbit coupling, was iterated to self-consistency but $\underline{\rho}'^n$ was taken to be spherically symmetric and diagonal in the total-energy expression (7), showed that for iron, cobalt, and nickel the second-order correction (in $\delta\underline{\rho}^n$) to the change in total energy was not larger than 2% of the first-order approximation $\Delta E(\hat{\mathbf{n}})$ (14), in agreement with the above estimate. However, we see that the second-order correction may be large compared to the MAE unless there is a systematic cancelation of contributions to the second-order terms for two different magnetization directions. That this may happen is at least plausible since such a systematic cancelation does occur for the first-order term. Before discussing the problem of the second-order terms the difference in single-particle eigenvalue sums must be calculated reliably and we address this problem next.

C. Aspects of the Brillouin-zone integration

In principle the force theorem establishes a simple intuitive relation between the density-functional theory band structure and the MAE. Within this framework the origin of the anisotropy energy may be understood in terms of the behavior of the energy bands in the Brillouin zone (BZ). In Sec. IV we will consider this in a detailed manner. Here we examine how densely $\varepsilon_i(\mathbf{k})$ and $\varepsilon_i(\hat{\mathbf{n}},\mathbf{k})$ must be sampled in order to calculate

$$\Delta E \equiv \Delta E(\hat{\mathbf{n}}_1,\hat{\mathbf{n}}_2)$$
$$= \Delta E(\hat{\mathbf{n}}_1) - \Delta E(\hat{\mathbf{n}}_2)$$
$$= \sum_{i,\mathbf{k}}^{\text{occ}} \varepsilon_i(\hat{\mathbf{n}}_1,\mathbf{k}) - \sum_{i,\mathbf{k}}^{\text{occ}} \varepsilon_i(\hat{\mathbf{n}}_2,\mathbf{k}) \tag{15}$$

with the required accuracy. A rough estimate of the number of $\mathbf{k}$ points required may be obtained as follows. A typical value for the d-band density of states at the Fermi level, ε_F, is $D(\varepsilon_F)\sim 10/4$ states/eV. If one were to assume that only the states at the Fermi level contributed to the MAE, then the number of electrons involved in contributing to ΔE would be $\Delta N = D(\varepsilon_F)\Delta E \sim 2.5\times 10^{-6}$ electrons. Thus for Fe or Ni a sampling density of approximately $(100)^3$ points per BZ would be required.

On rotating the magnetization direction $\hat{\mathbf{n}}$, there is a redistribution of the occupied energy bands in the Brillouin zone. This leads to a change in the value of the Fermi energy $\varepsilon_F(\hat{\mathbf{n}})$ (to ensure particle conservation) which is small, but in view of the size of the MAE not negligible. The difference in the Fermi energy between the [0001] and [10$\bar{1}$0] directions in cobalt is of order 10^{-4}

eV, and between the [001] and [111] directions in iron and nickel of order 10^{-6} eV. If a common Fermi energy for the two directions of magnetization were assumed, this would imply a difference in the number of particles, ΔN, between the two directions of magnetization of order 10^{-4} for cobalt and of order 10^{-6} for iron and nickel, erroneously contributing $(\Delta N)\varepsilon_F$ to the calculated MAE. From these considerations it is clear that the assumption of common Fermi energies for both magnetization directions, which is sometimes made in calculations where the shift in total energy is calculated through perturbation theory on the single-particle energies, is not justified.[39]

In terms of the density of states $D(\varepsilon,\hat{\mathbf{n}})$, the number of states $N(\varepsilon,\hat{\mathbf{n}})=\int^{\varepsilon}D(\varepsilon',\hat{\mathbf{n}})d\varepsilon'$ and the energy function $F(\varepsilon,\hat{\mathbf{n}})=-\int^{\varepsilon}N(\varepsilon',\hat{\mathbf{n}})d\varepsilon'$, the sum of single-particle energies $U(\hat{\mathbf{n}})$ may be written as

$$U(\hat{\mathbf{n}})=\int^{\varepsilon_F(\hat{\mathbf{n}})}d\varepsilon'\varepsilon'D(\varepsilon',\hat{\mathbf{n}})$$
$$\approx\varepsilon N(\varepsilon_F(\hat{\mathbf{n}}),\hat{\mathbf{n}})+F(\varepsilon,\hat{\mathbf{n}})+\tfrac{1}{2}(\varepsilon_F(\hat{\mathbf{n}})-\varepsilon)^2D(\varepsilon,\hat{\mathbf{n}}) \quad (16)$$

for an energy ε close to the Fermi energy $\varepsilon_F(\hat{\mathbf{n}})$. The difference in energy, $U(\hat{\mathbf{n}}_1)-U(\hat{\mathbf{n}}_2)$ can, to an excellent approximation, be replaced by the difference $F(\varepsilon,\hat{\mathbf{n}}_1)-F(\varepsilon,\hat{\mathbf{n}}_2)$ evaluated at a common energy ε close to $\varepsilon_F(\hat{\mathbf{n}}_1)$ and $\varepsilon_F(\hat{\mathbf{n}}_2)$, as the error involved is of order $(\varepsilon_F(\hat{\mathbf{n}}_1)-\varepsilon_F(\hat{\mathbf{n}}_2))(\varepsilon_F(\hat{\mathbf{n}}_1)+\varepsilon_F(\hat{\mathbf{n}}_2)-2\varepsilon)D(\varepsilon)$. This has been verified by explicit calculation. Relationship (16) is useful in combination with the linear analytic tetrahedron integration scheme.[40] Using this method the integrals over a single tetrahedron for the density of states, the number of states, as well as for the function $F(\varepsilon,\hat{\mathbf{n}})$ may be obtained analytically. This is more accurate than numerical integration and eliminates the energy mesh step $d\varepsilon$ as a convergence parameter,[41] which would have to be adjusted corresponding to the sampling density in the Brillouin zone.

In view of the extremely small energy differences we are interested in, attention must be given to the partitioning of the BZ. By using the point-group and translation symmetry of the lattice, the star of a $\mathbf{k}$ point can be determined defining an irreducible wedge of the Brillouin zone (IBZ). For a function with the symmetry of the lattice, such as $\epsilon(\mathbf{k})$, integration over the BZ is usually replaced by an integration over the IBZ. This integration is commonly performed by subdividing the IBZ into small tetrahedra.[40] However, it has been pointed out[42] that integration over all tetrahedra in the IBZ is *not* equivalent to integration over the tetrahedra in the BZ. Individual tetrahedra from the full BZ can be reduced using point-group and translation symmetry, but cannot, in general, be reduced to lie in the traditional IBZ. The use of that IBZ filled with tetrahedra misweights the boundary planes of the IBZ where the spin-orbit coupling has the largest effect, and thus we expect important deviations in the anisotropy energy obtained by this method if a sufficiently dense grid is not used. The convergence of the anisotropy energy may be affected by contributions from the boundaries of the IBZ. We have therefore used the procedure suggested in Refs. 42 and 43. Integrating over all tetrahedra in the zone can be exactly reduced to a weighted summation of integrations over irreducible tetrahedra. Filled bands are then integrated by the trapezoidal rule, which is known to be very efficient for functions which may be represented by a rapidly convergent Fourier series. In Sec. III A we compare the two integration methods. The accuracy needed can only be obtained if the mesh points used for the energy calculation of each field direction are equivalent, i.e., can be obtained from each other by one of the single group operations and thus are on the same lattice. Our calculational procedure results in vanishing anisotropy energies, if the exchange splitting or the spin-orbit coupling is set to zero or if the Fermi energy is above all bands (because the spin-orbit coupling operator is traceless).

D. LMTO-ASA implementation

By using the force theorem (14), the MAE can be obtained with an accurate description of the band structures $\varepsilon_i(\hat{\mathbf{n}},\mathbf{k})$. For the reasons mentioned earlier, we have chosen the LMTO method in the atomic-sphere approximation to determine the band structure. This method employs several approximations whose influence on the single-particle energies must be checked.

Firstly, in a partial wave expansion of the wave functions only a finite number, $l_{\max}$, of angular-momentum values is included. In transition metals augmenting a (*spd*) basis with $l_{\max}=2$ so as to include f partial waves leads to small changes in integrated quantities such as the spin and orbital moments. This is illustrated in Table I by our results for the magnetic moment and g factor. The f radial wave function is much less localized than the d radial wave function, and its inclusion provides for a better description of the regions of space in between atoms. The MAE was calculated both with $l_{\max}=2$ and $l_{\max}=3$. Although the convergence with respect to $l_{\max}$ can be improved by using the combined correction terms,[29] we have chosen not to use them because of the large number of structure constants required and because the convergence of the reciprocal-lattice sums required in their calculation is significantly slower than that required for the calculation of the regular structure constants.

Secondly, in the ASA the input potential is taken to be spherically symmetric within atomic spheres which replace the Wigner-Seitz cell. By means of a full-potential implementation[44] of the linear augmented plane wave (LAPW) method[29] we have checked the influence of nonspherical terms in the potential on the location and dispersion of the energy bands.

Thirdly, the energy-independent basis is only complete (for an atomic-sphere potential) for the arbitrary but fixed energy ε_ν. The energies, $\varepsilon_{\nu l\sigma}$, used to calculate the muffin-tin orbitals are usually chosen as the center of gravity of the occupied bands. By choosing $\varepsilon_{\nu l\sigma}=\varepsilon_F$ we have checked that this has a negligible effect on the calculated MAE.

Our LMTO basis states are the nearly orthogonal Θ

TABLE I. Spin and orbital magnetization (in μ_B/atom) of iron, cobalt, and nickel at experimental volumes. The basis set consists of *spd* or *spdf* partial waves. The experimental data were taken from Ref. 48.

		σ_z	l_z	m_z	g
Iron	*spd* (theory)	2.21	0.047	2.25	2.04
	spdf (theory)	2.16	0.048	2.20	2.04
	expt.	2.13	0.09	2.22	2.09
Cobalt	*spd* (theory)	1.61	0.085	1.70	2.11
	spdf (theory)	1.57	0.079	1.65	2.10
	expt.	1.59	0.16	1.75	2.19
Nickel	*spd* (theory)	0.63	0.054	0.69	2.17
	spdf (theory)	0.60	0.051	0.66	2.17
	expt.	0.56	0.05	0.62	2.18

functions devised by Andersen and Jepsen.[45,30] They have pure spin character, diagonalizing $\hat{\mathbf{n}}\cdot\sigma$. The radial wave functions are obtained by integration of the scalar-relativistic Schrödinger equation (2) with spin-up and spin-down potentials which are self-consistently calculated in the absence of spin-orbit coupling in a first step. The spin-orbit coupling is added to the Hamiltonian in a second step and the resulting generalized eigenvalue problem is reduced to standard form by Cholesky decomposition of the overlap matrix. The eigenvalues and eigenstates are then obtained by matrix diagonalization.

With this choice of two-component basis the exchange-field matrix is block-diagonal in spin, as is the overlap matrix. The spin-orbit coupling matrix contains the polar angles of the magnetization direction and the spin-orbit interaction parameters $\xi_{vl}^{\sigma\sigma'}$, $\dot{\xi}_{vl}^{\sigma\sigma'}$, and $\ddot{\xi}_{vl}^{\sigma\sigma'}$,[35] which are radial integrals of $\xi(r)$ with ϕ_{vl}^{σ} and $\dot{\phi}_{vl}^{\sigma}$, the partial wave $\phi_l^{\sigma}(\varepsilon,r)$ and its energy derivative $\dot{\phi}_l^{\sigma}(\varepsilon,r)=\partial\phi_l^{\sigma}(\varepsilon,r)/\partial\varepsilon$, respectively, evaluated at the energy $\varepsilon_{vl\sigma}$.[29]

E. Dipole-dipole anisotropy energy

An important contribution to the measured magnetic anisotropy of a sample, which we have not mentioned so far, is the shape anisotropy. This may be thought of as resulting from a classical magnetic dipolar interaction between magnetic moment densities $\mathbf{m}(\mathbf{r})$ (in units of μ_B, the Bohr magneton). The magnetostatic energy $E^{\text{dip-dip}}$ is (in a.u.)

$$E^{\text{dip-dip}}=\frac{1}{c^2}\int\int\frac{1}{|\mathbf{r}-\mathbf{r}'|^3}\left[\mathbf{m}(\mathbf{r})\cdot\mathbf{m}(\mathbf{r}')-3\frac{[(\mathbf{r}-\mathbf{r}')\cdot\mathbf{m}(\mathbf{r})][(\mathbf{r}-\mathbf{r}')\cdot\mathbf{m}(\mathbf{r}')]}{|\mathbf{r}-\mathbf{r}'|^2}d\mathbf{r}\,d\mathbf{r}'\right]. \tag{17}$$

In general, $\mathbf{m}(\mathbf{r})$ contains spin and orbital contributions. A multipole expansion of the magnetization density inside a single atomic sphere can be made with multipole moments $\mathbf{m}_{lm}=\int r^l Y_{lm}^*\mathbf{m}(\mathbf{r})d\mathbf{r}$. The interatomic contribution to (17) associated with the $l=0$ multipole moment of the density, $\mathbf{m}_{00}=(4\pi)^{-1/2}\mathbf{m}_\tau$, is (per unit cell)

$$\frac{1}{c^2}\sum_{\mathbf{R},\tau,\tau'}{}'\frac{1}{|\mathbf{R}+\tau-\tau'|^3}\left[\mathbf{m}_\tau\cdot\mathbf{m}_{\tau'}-3\frac{[(\mathbf{R}+\tau-\tau')\cdot\mathbf{m}_\tau][(\mathbf{R}+\tau-\tau')\cdot\mathbf{m}_{\tau'}]}{|\mathbf{R}+\tau-\tau'|^2}\right], \tag{18}$$

where τ denotes the atom positions within one unit cell and $\mathbf{m}_\tau$ is the total magnetic moment in an atomic sphere around site τ.

Due to the long range of the magnetic dipole-dipole interaction, the integral (17) depends on the shape of the sample and this leads to shape anisotropy. The discrete dipole sum in (18), which in three dimensions is only conditionally convergent, may be treated by Ewald-summation techniques.[46] If the term with $\mathbf{G}=\mathbf{0}$ in the reciprocal space part of the summation is omitted, then the remainder is absolutely convergent.[47] The latter does not give rise to any anisotropy energy in monatomic cubic lattices, and the multipole expansion would have to be carried out to higher order to obtain contributions to the anisotropy energy. In Fig. 1, the variation of the anisotropy energy $[E^{\text{dip-dip}}(0001)-E^{\text{dip-dip}}(10\bar{1}0)]$ derived from the dipole sum (18) for an hcp lattice as a function of the c/a ratio at a constant volume, is shown. $E^{\text{dip-dip}}(\hat{\mathbf{n}})$ is the dipole sum in (18) with all the dipoles oriented along the $\hat{\mathbf{n}}$ direction. The magnetic moment per site, $|\mathbf{m}_\tau|$, has been taken to be $1.7\mu_B$ (approximately the magnetic moment of cobalt) and the volume corresponds to the exper-

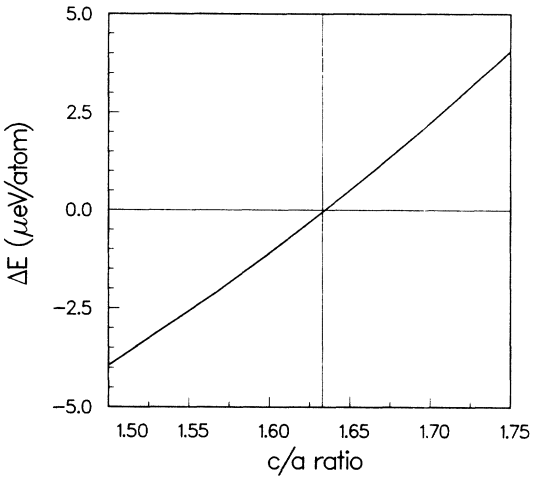

FIG. 1. Contribution of the dipole-dipole sum (18) to the magnetocrystalline anisotropy energy in a hcp lattice as a function of the c/a ratio. The magnetic moment per site has been taken to be $1.7\mu_B$ and the volume corresponds to a Wigner-Seitz sphere radius of 2.621 a.u. A vertical line marks the ideal ratio $c/a=\sqrt{\frac{8}{3}}$.

imental volume of cobalt (Wigner-Seitz sphere radius $S=2.621$ a.u. The unit of length in atomic units is the Bohr radius, $a_0=0.529$ Å). It can be inferred from the figure that the anisotropy energy arising from the dipole-dipole sum (18) is almost completely a consequence of the difference between the actual c/a ratio and its ideal value $\sqrt{\frac{8}{3}}$. Cobalt has a c/a ratio which deviates only -0.67% from the ideal value and we retain a value of 0.4 μeV/atom favoring the c axis.

The contribution of higher multipole moments $\mathbf{m}_{lm}$ to the magnetostatic energy will be a factor $\sim(m_{lm}/m_{00})(m_{l'm'}/m_{00})$ smaller than the dipole-dipole energy (18). The next nonzero moment in uniaxial cobalt is a quadrupole moment ($l=2$), and in cubic iron and nickel an octupole moment ($l=4$). A full potential calculation results in a quadrupole moment for cobalt such that $m_{2m}/m_{00}\sim 10^{-4}a_0^2$ and in an octupole moment for nickel such that $m_{4m}/m_{00}\sim 10^{-2}a_0^4$. These small moments reflect the small deviation of the charge density in the muffin-tin spheres from spherical symmetry. We expect the contributions to the magnetostatic energy from higher multipoles to be correspondingly smaller than the value for the dipole-dipole sum calculated above and thus entirely negligible.

Inclusion of spin-orbit coupling leads to anisotropy in the magnetization and to a deviation of the local direction of the magnetization from the average (z) magnetization direction, i.e., $m_x(\mathbf{r})$ and $m_y(\mathbf{r})$ are no longer zero. The intra-atomic magnetostatic energy per atom is of order $E^{\text{intra}}=m^2/c^2S^3$. With $m=|\mathbf{m}_r|=1.7\mu_B$ and $S=2.6$ a.u. this yields 30 μeV in cobalt. As the magnetization is anisotropic by an amount Δm, the intra-atomic magnetostatic energy is anisotropic by an amount $2(\Delta m/m)E^{\text{intra}}$. In cobalt, $\Delta m/m=4.5\times10^{-3}$,[48] and this results in a contribution to the MAE which is less than 1% of the measured value. In iron and nickel, $\Delta m/m=7.8\times10^{-5}$ and 18×10^{-5}, respectively,[48] and this leads to very small contributions to the MAE as well. We conclude that the MAE of iron, cobalt, and nickel does not have its origin in the magnetostatic energy.

III. CALCULATIONS

The problem of calculating the single-particle eigenvalue sum to one part in 10^7 and the convergence of the Brillouin-zone integral are discussed in Sec. III A. In Sec. III B we investigate how the calculated ΔE depends on the number of partial waves included in the angular-momentum expansion of the wave functions.

A. Convergence of the Brillouin-zone integral

The energy difference $\Delta E=\Delta\int\varepsilon D(\varepsilon)d\varepsilon$ is calculated as described in Sec. II. After diagonalizing the Hamiltonian including the spin-orbit coupling term, the bands are filled with electrons up to the Fermi energy ε_F, defined so that $1/\Omega_{\text{BZ}}\int^{\varepsilon_F}\int_{\text{BZ}}\sum_l\delta(\varepsilon-\varepsilon_l(\mathbf{k}))d^3\mathbf{k}d\varepsilon=\int^{\varepsilon_F}D(\varepsilon)d\varepsilon=n$, the number of valence electrons per atom. Ω_{BZ} is the Brillouin-zone volume. The single-particle eigenvalue sum, $\int^{\varepsilon_F}\varepsilon D(\varepsilon)d\varepsilon$, is calculated using this Fermi energy. To see how sensitive ΔE is to details of the band structure, we also calculate ΔE for a range, δn, of noninteger fillings about n using the band structure calculated self-consistently for n electrons. We denote this auxiliary function as $\Delta E^n(q)$, where $q=n+\delta n$. We will use $\Delta E\equiv\Delta E^n(n)$.

The resulting function $\Delta E^n(q)$ is shown in Figs. 2–4 for Ni, Co, and Fe, respectively. For Ni the results of calculations of $\Delta E^n(q)$ with three different Brillouin-zone

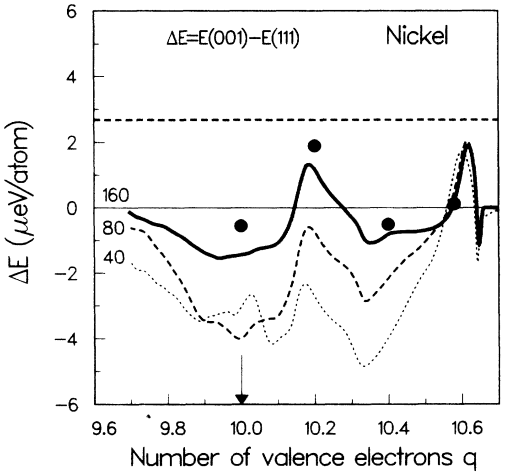

FIG. 2. The magnetocrystalline anisotropy energy as a function of the number of valence electrons, $\Delta E^n(q)$, calculated with the band structure of Ni, $n=10$. $q=n$ is indicated by an arrow. The experimental value is indicated by the horizontal dashed line; converged calculated values, as discussed in the text, are denoted by a solid circle. The dotted, dashed, and solid curves are obtained from calculations with 40, 80, and 160 divisions along a reciprocal lattice vector, using an *spd* basis.

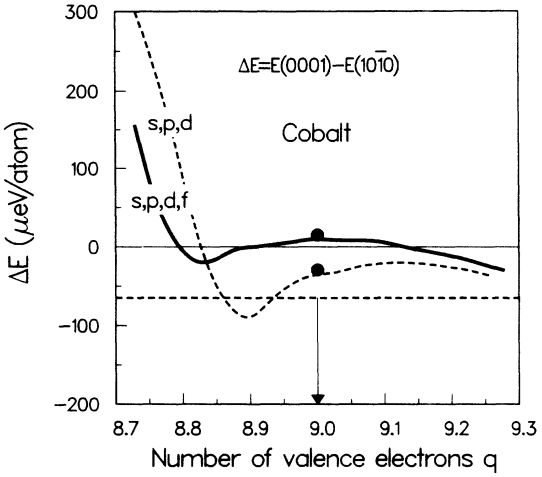

FIG. 3. $\Delta E^n(q)$ for Co, $n=9$. $q=n$ is indicated by an arrow. The dashed curve was obtained from a band structure calculated with an *spd* basis. The solid curve was obtained from a band structure calculated with an *spdf* basis. The experimental value is shown as a horizontal dashed line. Converged calculated values are shown as solid circles.

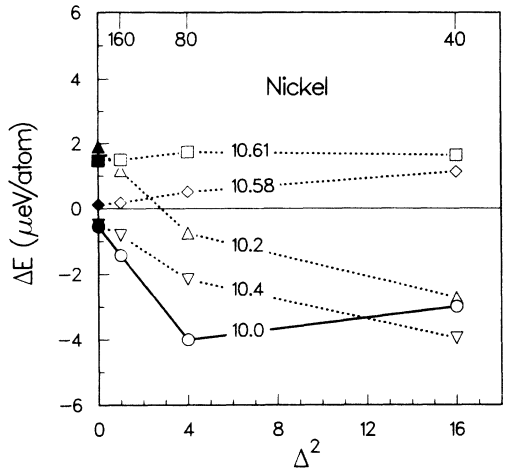

FIG. 5. Convergence of $\Delta E^n(q)$ for $n=10$ and several selected values of q as a function of the scaled tetrahedron surface area Δ^2. $\Delta=(v/v_0)^{1/3}$, where v is the volume of a tetrahedron and v_0 is the volume of a tetrahedron obtained by dividing the reciprocal lattice vectors into 160 intervals. The number of divisions of the reciprocal lattice vectors used in the calculations, N, is indicated at the top of the figure. The results obtained with the adaptive integration scheme described in the text are denoted by the solid symbols on the vertical axis.

meshes corresponding to $N=40$, 80, and 160 divisions of the reciprocal-lattice vectors are shown. Although the form of $\Delta E^n(q)$ may be obtained with a moderately fine mesh, it is not at all clear from Fig. 2 that it is adequately converged even with the mesh corresponding to 160 divisions. For bands whose dispersion within a tetrahedron is quadratic in $\mathbf{k}$, the linear analytic tetrahedron method gives rise to an error in the single-particle eigenvalue sum which is proportional to $v^{2/3}$. (v, the volume of a single tetrahedron, is equal to $\Omega_{BZ}/6N^3$.) Part of this error comes from filled tetrahedra[43] and part from partially filled tetrahedra which the Fermi surface intersects. Although it has been demonstrated in a few cases[43] that the error arising from the filled tetrahedra dominates that arising from the partially filled tetrahedra on the scale of millielectronvolts, it is not *a priori* obvious that the latter error can be neglected in a calculation of ΔE on a microelectronvolt scale.

The anisotropy energy $\Delta E^n(q)$ is plotted as a function of $v^{2/3}$ in Fig. 5 for a few representative values of $q=10.0$, 10.2, 10.4, 10.58, and 10.61. For some values of q it seems to be possible to extrapolate the calculated values of $\Delta E^n(q)$ to an infinitely dense mesh ($v\to 0$) whereas for other values of q, and in particular for $q=10.0$, the convergence is not very systematic. By examining the tetrahedra where the convergence is slow, we have found that the origin of this problem lies in the band crossings and anticrossings which occur near the Fermi energy close to X (Fig. 6) along what were high symmetry lines in the absence of spin-orbit coupling. These give rise to the deviations from a straight line seen in Fig. 5. (In particular, the d-hole pocket Fermi surface is sensitive to the magnetization direction.) In Fig. 6, mesh points corresponding to 40, 80, and 160 divisions of the reciprocal-lattice vectors are shown together with the bands in the region close to the Fermi energy. It is clear that 40 divisions do not resolve the band crossings at all adequately while the 80 and 160 division meshes begin to resolve individual band crossings of the five bands which cross the Fermi energy within a distance of $0.025(2\pi/a)a_0^{-1}$ of each other. A mesh of $(160)^3$ points is the densest uniform mesh for which we were able to perform a calculation for Ni. Even making full use of symmetry,[42] this required diagonalizing an 18×18 Hamiltonian at $\sim 550\,000$ $\mathbf{k}$ points.

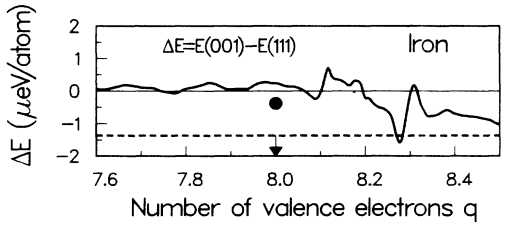

FIG. 4. $\Delta E^n(q)$ for Fe, $n=8$. $q=n$ is indicated by an arrow. The experimental value is shown by the horizontal dashed line; the converged calculated value is denoted by a solid circle. The solid curve was obtained from calculations with 96 divisions along a reciprocal lattice vector using an *spd* basis.

Because the integrand is, in general, not smooth (see Fig. 6) we choose to subdivide our original mesh ($N\to 2N$) rather than taking another mesh with a slightly different interval N'. If we did this, or if we simply displaced the original mesh by a fraction of an interval, then we would obtain another value for ΔE and the variance of these results would be a measure of the error in the integration. This is illustrated in Fig. 7 for Ni, where ΔE is shown as a function of the tetrahedron volume for a large range of volumes and using a uniform mesh. The corre-

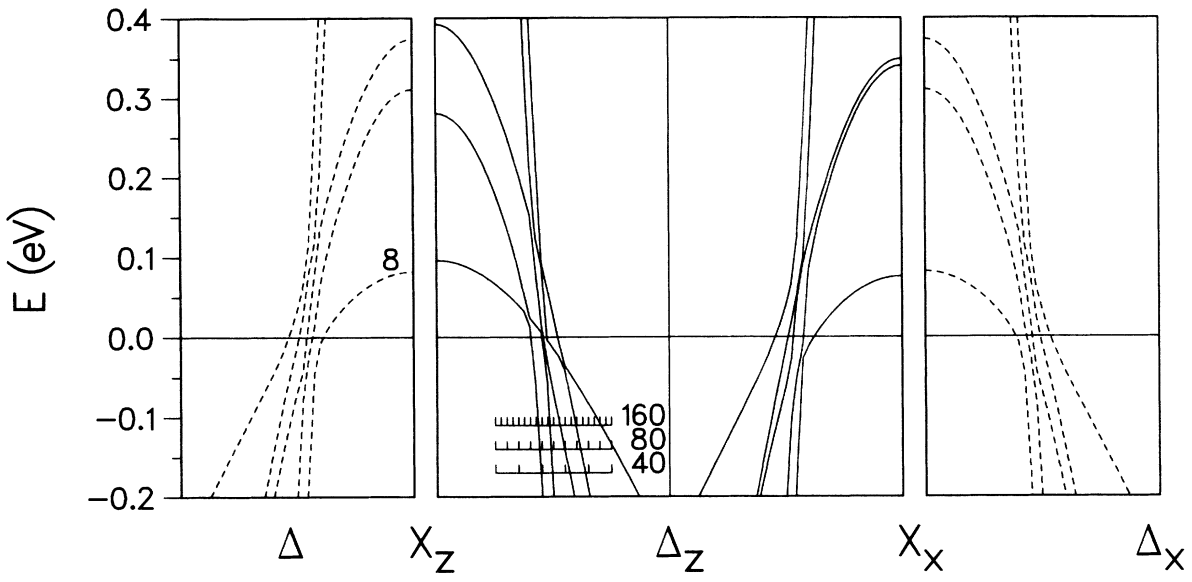

FIG. 6. Band structure of Ni along $\Delta_z = 2\pi/a(0,0,l)$ and $\Delta_x = 2\pi/a(l,0,0)$ with the spin quantization axis in the (111) (dashed lines) and (001) (solid lines) directions. Here $0.5 \leq l \leq 1.0$. $l = 1.0$ corresponds to the X point. Division of the reciprocal lattice vectors into 40, 80, and 160 intervals is indicated in the figure. The Fermi level corresponding to 10 electrons per atom is chosen as the zero of energy.

sponding number of divisions, N, of the reciprocal-lattice vectors is shown at the top of the figure.

For almost all of the meshes considered ΔE is seen to be negative. If the irreducible wedges with incorrect weighting are used, then the ΔE obtained is that shown by the open diamonds in Fig. 7. It is evident that, for such coarse meshes, the misweighting has a large effect on the calculated values and that it is possible to find

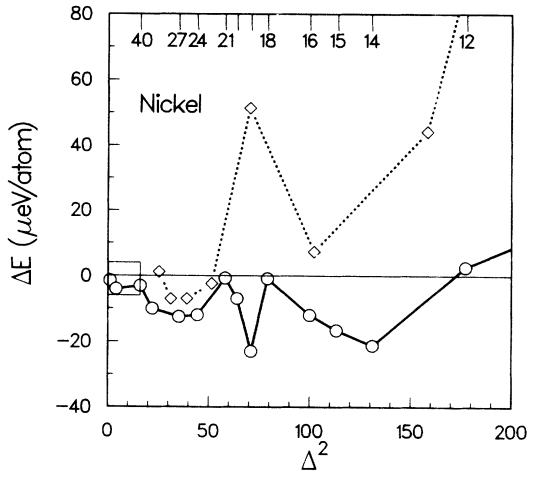

FIG. 7. MAE for Ni ($n = 10$) obtained with coarse integration meshes. ΔE is plotted as a function of Δ^2 where $\Delta = 160/N$ (see Fig. 5) and N, the number of intervals along the reciprocal lattice vectors used in the Brillouin-zone integration, is shown at the top of the figure. Results obtained by integration over irreducible wedges (diamonds) are connected by a dashed line; results obtained by integration over the Brillouin zone of the fcc lattice with correct weighting of sampling points (circles) are connected by a solid line. The data in the small box at the origin are shown on an expanded scale in Fig. 5.

mesh densities where the calculated value for ΔE is in (fortuitously) good agreement with experiment.

Because the convergence problems are associated with band crossings and anticrossings near the Fermi energy, a very dense uniform mesh is not necessary. (If the partner bands involved in a crossing or anticrossing are either both occupied or unoccupied, then the errors cancel and no problem occurs.) At a band crossing, $\varepsilon_i(\mathbf{k})$ is not differentiable so that the use of interpolation schemes to generate the function on a dense mesh will in general not be helpful. We have therefore developed an adaptive integration scheme which refines tetrahedra that are particularly difficult to converge at a chosen Fermi energy by subdividing them into eight smaller tetrahedra. These eight tetrahedra are themselves subdivided until the required accuracy is achieved. For those tetrahedra where the convergence is smooth (i.e., $\propto v^{2/3}$) we use a local quadratic expansion of the bands to extrapolate (analytically) the contribution to the anisotropy energy to zero volume (infinitely dense mesh). A limit is set in practice by the amount of memory available on our computer (an IBM model 3090 computer with 128 Mbytes of core storage). The results obtained with this method are marked as solid symbols along the vertical axis in Fig. 5 and as solid circles in Figs. 2–4. These values represent estimates for the results obtained by extrapolating the values obtained with $N = 80$ and 160 (open symbols) assuming a $v^{2/3}$ dependence. The calculation was, however, a factor ~ 6 faster than the calculation performed with the uniform mesh of $(160)^3$ points. This value of ΔE, representing our best estimate for the anisotropy energy for Ni, is given in Table II. In order to make an estimate of the error bar on this value, we performed calculations based on slightly different meshes which sample the band crossings in Fig. 6 differently. From these other

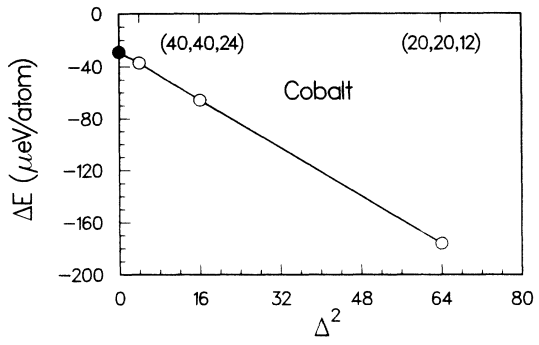

FIG. 8. Convergence of ΔE for Co as a function of Δ^2. $\Delta=(v/v_0)^{1/3}$, where v is the volume of a tetrahedron and v_0 is the volume of a tetrahedron corresponding to 160 divisions of the reciprocal lattice vectors in the (x,y) plane and 96 divisions of the reciprocal lattice vector along the z axis.

values we estimate the accuracy to be ± 0.5 μeV for Fe and Ni.

For Co we found the convergence of $\Delta E(q)$ to be very regular for all values of q shown in Fig. 3. In Fig. 8, $\Delta E[\equiv \Delta E^n(n)]$ is plotted as a function of $v^{2/3}$ for three different meshes (open circles). These calculations were performed with an *spd* basis set. The coarsest mesh has $N_c=12$ divisions of the reciprocal-lattice vector in the z direction and $N_a=20$ divisions of the reciprocal-lattice vectors in the basal plane. We denote this mesh by (20,20,12). By doubling the number of divisions in each direction the second (40,40,24) and third (80,80,48) meshes are obtained. The iterative refinement scheme leads to a value for ΔE of -29 μeV (solid circle). The deviation of the open circles from a straight line indicates an error bar of ± 2 μeV. In order to test the sensitivity to the details of the sampling, ΔE was calculated for several other meshes similar in density to the (40,40,24) mesh. The error bar derived from these calculations is consistent with that just given. The values for ΔE given in the tables were obtained from the iterative refinement calculation.

B. Convergence with respect to the number of partial waves

Before discussing the results, we first consider the effect on ΔE of truncating the angular-momentum expansion of the wave functions at some $l_{\max}$ (Sec. II D). Self-consistent spin-polarized calculations were first performed with basis sets containing *spd* ($l_{\max}=2$) and *spdf* ($l_{\max}=3$) partial waves. For Co the resulting band structures are plotted along symmetry lines in the *AHL* plane in Figs. 9(a) and 9(b), respectively. Including spin-orbit coupling and with the field along the c axis the bands are as shown in Fig. 9(c). ΔE was then determined for each of the two basis sets using the adaptive integration scheme described above. The results for Fe, Co, and Ni ($n=8$, 9, and 10 electrons, respectively) are given in Table III and for Co, $\Delta E^n(q)$ as calculated with both values of $l_{\max}$ is shown in Fig. 3. The difference between ΔE obtained with $l_{\max}=2$ and $l_{\max}=3$ is small for Fe and Ni, but large for Co, where with the *spd* basis the c axis is found to be the easy axis, in agreement with experiment.[16] With the *spdf* basis the easy axis is found to be in the basal plane and the absolute value of the anisotropy energy is reduced to ~ 15 μeV/atom. Because of the

TABLE II. Magnetocrystalline anisotropy energy, ΔE, in μeV/atom for Fe, Co, and Ni. ΔE was calculated at the experimental volume with two basis sets of LMTO's for which $l_{\max}=2$ and $l_{\max}=3$, respectively. The numerical uncertainty in the anisotropy energy is estimated to be 0.5 μeV for Ni and Fe, and about 2 μeV for cobalt. The experimental values of the MAE for Co were taken from Ref. 3 and for Fe and Ni from Ref. 4.

	Fe $E_{001}-E_{111}$	Co $E_{0001}-E_{10\bar{1}0}$	Ni $E_{001}-E_{111}$
spd	−0.4	−29	−0.6
spdf	−0.5	16	−0.5
expt.	−1.4	−65	2.7

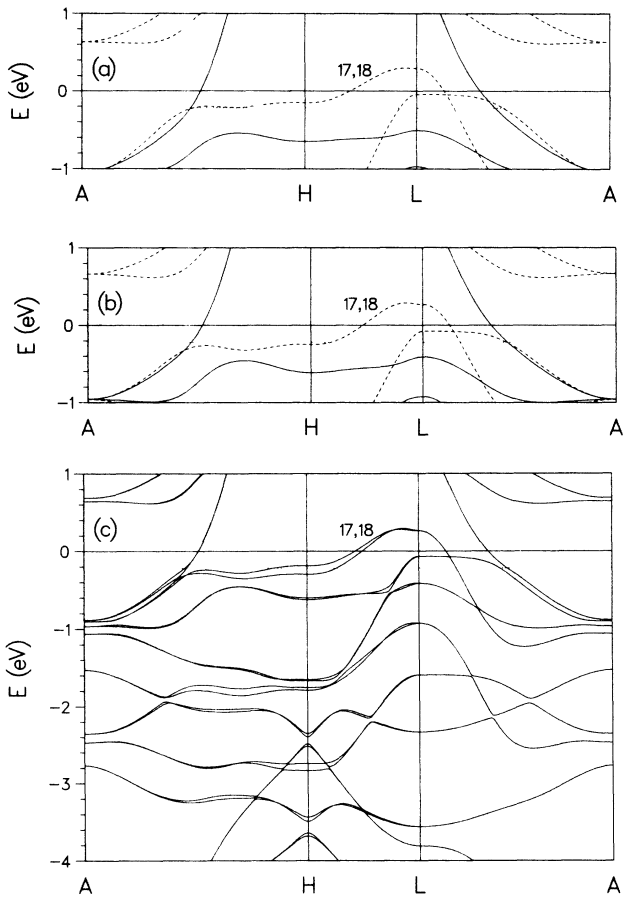

FIG. 9. Co band structure along symmetry lines in the *AHL* plane. (a) Calculation performed without spin-orbit coupling with an *spd* basis. (b) Calculation performed without spin-orbit coupling with an *spdf* basis. Solid curves are majority bands, dashed curves are minority bands. The zero of energy, chosen to correspond to a filling of $q=9$ electrons per atom, is shown as a horizontal line. The Fermi energy corresponding to a filling of 8.8 valence electrons is denoted by the dashed horizontal line. (c) Calculation performed including spin-orbit coupling with an *spdf* basis with the spin quantization axis along (0001).

small amplitude of the f partial wave near the nucleus, the f-wave spin-orbit coupling parameter is 2 orders of magnitude smaller than the spin-orbit coupling parameter for the d partial waves. This is not the cause of the change in ΔE. Examination of the local anisotropy energy in the Brillouin zone showed that the difference originates completely from a change in the electronic structure in a slab of total thickness $2\pi/6c$ around the AHL plane.

The most important difference between Figs. 9(a) and 9(b), which we identify as giving rise to the change in $\Delta E^n(q)$ seen in Fig. 3, is that the inclusion of f partial waves leads to bands 17 and 18 being pushed downwards (by 0.09 eV with respect to the Fermi energy at point H and by 0.11 eV, three-quarters of the way along line AH) decreasing the volume of the hole pocket around point L.

To determine whether the LMTO-ASA band structure for Co was sensitive to further changes in the basis or to details of the potential not captured by the ASA, we performed spin-polarized full-potential LAPW (FLAPW) calculations for Co. Compared with the band structure shown in Fig. 9(b) we found that in the FLAPW calculation bands 17 and 18 lie at most 0.03 eV higher along line AH. We therefore expect the MAE calculated with a full-potential method to be intermediate between the *spd* and *spdf* results shown in Fig. 3. ΔE will thus not be changed by as much as is needed to bring it into agreement with experiment.

IV. RESULTS

One of the aims of the present investigation was to determine whether any trends in ΔE could be identified as a function of the bandwidth, the strength of the spin-orbit coupling, or of the band filling (number of valence electrons). In a preliminary study based on canonical bcc, fcc, and hcp bands,[34] no simple trends were found for reasonable values of the spin-orbit coupling parameter, exchange-splitting, and $3d$ bandwidth. This may be different if the bandwidth is of order of the spin-orbit splitting.[49] We found that there were contributions to the anisotropy energy from both states near the Fermi level (which in the absence of spin-orbit coupling were degenerate) giving rise to a Fermi-surface-dependent contribution as well as from states that are completely filled which give rise to a Fermi-surface-independent contribution. Both contributions may be of the same order of magnitude and may have opposite sign. This has previously been discussed in detail for nickel.[11] The completely filled states are relatively easy to understand. If they are degenerate in the absence of the spin-orbit interaction, they can be split by this interaction in first order. To first order in ξ these splittings are of equal magnitude but opposite sign and hence make no contribution to ΔE. There are noncanceling higher-order contributions to ΔE arising from interactions of the occupied with the unoccupied states. The contribution to the anisotropy energy left over after summing over all single-group symmetry-related $\mathbf{k}$ points scales with ξ^2 for hexagonal lattices, and ξ^4 for cubic lattices. The expression for the anisotropy energy thereby obtained is strictly only valid when, for the band being considered, all $\mathbf{k}$ points related by single-group symmetry are occupied. In that case the anisotropy energy scales with the expected power of ξ.[50] However, close to the Fermi energy the simultaneous occupation of all $\mathbf{k}$ points for a band is not guaranteed, especially not if the band was degenerate, thereby destroying the simple dependence on ξ. The trends that otherwise might be present can be obscured by this Fermi-surface-dependent contribution.

In Sec. IV A we discuss the origin of the calculated ΔE and in Sec. IV B we show how ΔE depends on small changes in the number of electrons. In Secs. IV C–IV E the dependence of ΔE on the strength of the spin-orbit coupling, the lattice strain, and the choice of exchange-correlation potential, respectively, is examined.

A. Anisotropy energy of Fe, Co, and Ni

1. Nickel

Although the maximum splitting of the energy bands when spin-orbit coupling is introduced is of the order of $\frac{5}{2}\xi_d$ (where ξ_d is the free-atom spin-orbit coupling parameter), ΔE is much smaller than this. One reason for this is that the number of electrons whose energy is lowered by the full spin-orbit splitting is very small because the coupling is only effective around points and lines of high symmetry. The other reason is that in reciprocal space there is a partial cancelation of anisotropy contributions from different regions in the Brillouin zone which would be equivalent without spin-orbit coupling. To illustrate this, part of the band structure of Ni along the lines Γ–$X(001)$ and Γ–$X(100)$ near the X point is shown in Fig. 6 for two different magnetization directions $\hat{\mathbf{n}}\|[001]$ and $\hat{\mathbf{n}}\|[111]$. As a rule of thumb, the spin-orbit splitting is largest for $\mathbf{k}\|\hat{\mathbf{n}}$ and smallest for $\mathbf{k}\perp\hat{\mathbf{n}}$.[51] By comparing the (001) and (111) energy bands at both X points, we see that compensating contributions can be expected. This is indeed found in the detailed calculations. By plotting the anisotropy energy density in reciprocal space we find that the *changes* in $\Delta E^n(q)$ shown in Fig. 2 may be attributed to bands close to ε_F whose degeneracy along lines of high symmetry is lowered by the inclusion of spin-orbit coupling, i.e., $d\Delta E^n(q)/dq$ is a Fermi-surface-related effect. To understand the absolute value of $\Delta E^n(q)$, the contribution from all the filled bands must be included (or, if we work in terms of holes, all the unfilled bands). Because the spin-orbit operator is a traceless operator, the anisotropy energy is zero once the Fermi level is above the d-band complex. In nickel this has the consequence that only states near points L and X contribute to the anisotropy.

From Fig. 2 it is clear that the calculated ΔE has the wrong sign in nickel. It can also be seen that a maximum occurs in the anisotropy energy at about 10.2 electrons. For this occupation the Fermi level is near the top of band 8 at point X. de Haas–van Alphen (dHvA) measurements[51] have failed to find any orbits with the extremal area predicted for this hole pocket by LSDA calculations.[52] In measurements of the magnetic anisotropy, the large number of Fourier coefficients needed to describe the torque has been interpreted as being due to the presence of a much smaller pocket than predicted by the

LSDA, which is populated and depopulated when the magnetization direction is changed and the top of band 8 moves through ε_F.[53]

Our analysis of $\Delta E^n(q)$ indicates that a shift of band 8 downwards such that the hole pocket is almost completely eliminated would lead to a positive $\Delta E^n(q)$ around $q=10$. It is tempting to speculate that the correction to the LSDA necessary to bring the density-functional Fermi surface into agreement with dHvA would also lead to a ΔE in agreement with experiment. However, this assumes that the true Fermi surface would be given by the density-functional single-particle eigenvalues. Recently it has been shown by counterexamples that this cannot be expected to be true in general.[54]

2. Cobalt

From Fig. 3 (solid curve, calculated with $l_{\max}=3$) it can be seen that, for cobalt, the calculation does not predict the correct easy axis. In the absence of spin-orbit coupling, the whole *AHL* plane is doubly degenerate for each spin due to the screw operation in the hcp lattice. Depending on the direction of the magnetization this double degeneracy may be removed when spin-orbit coupling is added. From group theory one finds that the bands in the *AHL* plane remain doubly degenerate with $\hat{\mathbf{n}}$ perpendicular to the c axis.[55] This degeneracy is removed if $\hat{\mathbf{n}}$ is parallel to the c axis (except along the line *AL* which remains doubly degenerate). This group-theoretical result was confirmed in the numerical calculation. The resulting band structure along symmetry lines in the *AHL* plane is shown in Fig. 9(c). The Fermi surfaces in the *AHL* plane using the bands calculated with $l_{\max}=3$ are shown in Figs. 10 and 11 for $\hat{\mathbf{n}}$ parallel and perpendicular to the c axis, respectively.

From these symmetry considerations a large contribution to ΔE might be expected from a region around the whole two-dimensional *AHL* plane. In particular, we expect a large anisotropy if there are doubly degenerate bands with little dispersion at the Fermi level so that the spin-orbit coupling can cause one of the bands to become completely filled and the other to become completely empty. This criterion is obviously fulfilled for the Fermi energy corresponding to ~ 8.75 electrons in Figs. 9(b) and 9(c). (The dashed horizontal line shown in the figure corresponds to a filling of 8.8 electrons). This structure accounts for the very rapid *change* in $\Delta E^n(q)$ at $q=8.75$ whose onset occurs at $q\sim 8.8$ in Fig. 3.

The exact location and dispersion of the degenerate bands 17 and 18 in the *AHL* plane with respect to the Fermi level thus influence the calculated ΔE very strongly. At the L point of the zone these bands have almost equal p-like and d-like character whereas at the H point the character is almost completely d-like. Both the dispersion and the location with respect to the Fermi level of these two bands can change upon inclusion of free-electron-like f states in the basis (Fig. 9). As seen in Sec. III B, bands 17 and 18 are shifted downwards at H by 0.09 eV with respect to ε_F and the Fermi-surface dimensions of these bands in the *AHL* plane become smaller upon inclusion of f states in the basis.

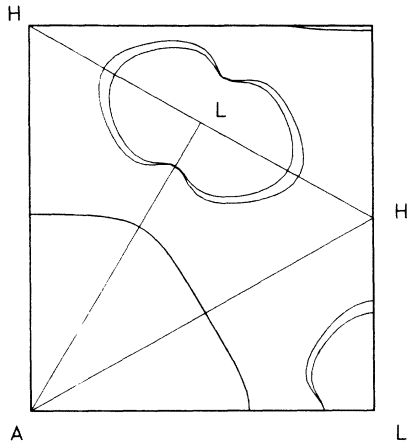

FIG. 10. Fermi surface for Co in the *AHL* plane with the field along (0001), corresponding to the band structure shown in Fig. 9(c). The splitting of bands 17 and 18 around L is due to the spin-orbit coupling and gives rise to the large variation of $\Delta E^n(q)$ around $q=8.75$ electrons in Fig. 3.

3. Iron

In iron the correct sign is obtained for ΔE and the function $\Delta E^n(q)$ (Fig. 4) is featureless for values of $q\sim 8$. However, in view of the results for Ni and Co this agreement with experiment must be regarded as being fortuitous.

B. Number of valence electrons

By forming a very dilute alloy it should be possible to probe the sensitivity of the anisotropy energy to the band structure in the neighborhood of ε_F for the elemental materials. In Ni a rapid decrease of anisotropy energy on alloying both with Cu, Rh, and Ru is experimentally observed at low temperatures.[48] At room temperature, alloying with Co and Fe also leads to a decrease.[48] For Co we have not found any low-temperature measurements. A slight decrease in the anisotropy energy at 77 K has

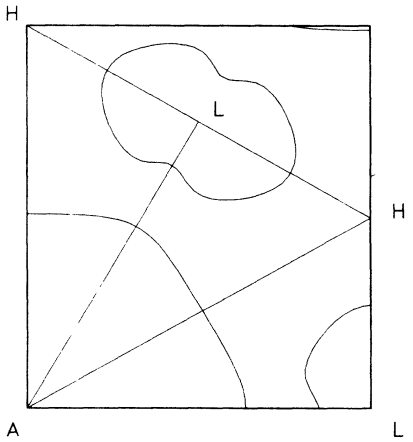

FIG. 11. Fermi surface for Co in the *AHL* plane with the field along $(10\bar{1}0)$, from a calculation performed with an *spdf* basis. Bands 17 and 18 are not split by the spin-orbit interaction if the spin quantization axis is perpendicular to the c axis.

been reported on alloying Co with Ni.[48] At room temperature alloying Co with Fe also leads to a decrease in the anisotropy.[48]

Because we do not predict the correct easy axis for Co or Ni, a detailed comparison with experiment is not possible. It is nevertheless of interest to know the range of validity of the function $\Delta E^n(q)$. The large variations found in $\Delta E^n(q)$ for Ni and Co (Figs. 2 and 3) occurred for values of q outside the range $|q-n|<\xi/I_{xc}\sim 0.05$, where $d\Delta E^n(q)/dq$ may be considered reliable. Outside this small range of δn the exchange splitting $\Delta\varepsilon_{xc}$ can no longer be regarded as being constant. According to the well-known Slater-Pauling curve, the magnetic moment decreases linearly with increasing number of valence electrons and in general the exchange splitting is proportional to the magnetic moment, $\Delta\varepsilon_{xc}=mI_{xc}$. The Stoner parameter, I_{xc}, may be taken to be constant over the range of δn we are interested in. For a given number of valence electrons q, the exchange splitting and the magnetic moment must be determined self-consistently. The simplest way of doing this is within the virtual-crystal approximation (VCA). For dilute alloys formed with neighboring elements in the common band regime, the VCA should be a reasonable guide to the alloying behavior of the MAE. For sufficiently high alloy concentration the effect of disorder will be to smear out the Fermi surface and the VCA will break down. We have carried out self-consistent spin-polarized calculations for noninteger numbers of valence electrons, $n+\delta n$, such that $n=9$ or 10, corresponding to Co and Ni, respectively, and $\delta n=-0.2$, -0.1, 0.0, 0.1, and 0.2 electrons for Co and $\delta n=0.0$, 0.1, 0.2, and 0.3 electrons for Ni. For these calculations the experimental Co and Ni lattice constants were used.

The values of $\Delta E\equiv\Delta E^{n+\delta n}(n+\delta n)$ shown in Fig. 12 as solid symbols were calculated as previously for integer values of n using the iterative refinement scheme. The open symbols represent values of $\Delta E^{n+\delta n}(q)$ also obtained with the iterative refinement scheme but for different filling ($q\neq n+\delta n$) of the self-consistently calculated ($n+\delta n$) band structure. The solid symbols follow the trend indicated by the heavy line, $\Delta E^n(q)$, in Fig. 12. There is a minimum in the anisotropy energy at $q=10$ electrons and a maximum around $q=10.2$ electrons. However, there are quantitative differences, the most obvious of which is that within the VCA the MAE corresponding to 10.2 electrons is now *larger* than the experimental value. The origin of this peak is related to the band-8 hole pocket at point X and underlines the necessity to describe this feature correctly. The existence of such a peak would provide a natural explanation for the observed rapid decrease in MAE when Ni is alloyed with either Cu, Rh, or Ru.[48] Although the uncertainty related to the existence of the X hole pocket discussed in the previous section remains, it seems highly likely that band 8 at point X will be shifted downwards with respect to the other bands in a full density-functional calculation. The results shown in Fig. 12 indicate that the function $\Delta E^{n+\delta n}(q)$ provides a good description of the MAE over a range of $|q-n|<0.05$ electrons, in agreement with the estimate given above.

For Co the VCA results, $\Delta E^{n+\delta n}(n+\delta n)$, shown as circles in Fig. 13, track the $\Delta E^n(q)$ curve remarkably faithfully and much better than we had expected. The reason is simple. The majority-spin d bands are completely filled in Co (i.e., it is a strong ferromagnet) and the exchange splitting is large compared to the spin-orbit interaction parameter. There are therefore no majority-spin bands close to the bands at the Fermi energy which can be coupled to by the spin-orbit interaction. For a small change in the number of valence electrons, the topology of the minority bands around the Fermi energy corresponding to a given filling of the energy bands does not change nor can it change significantly when the spin-orbit interaction is switched on. It is this topology which determines the anisotropy energy. The large basal plane anisotropy for $q<8.8$ electrons indicated by $\Delta E^n(q)$ is confirmed by the VCA calculation. However, we have

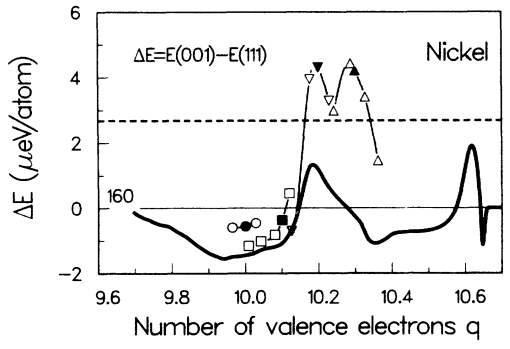

FIG. 12. $\Delta E^{n+\delta n}(q)$ calculated with an *spd* basis for $n+\delta n=10.0$ (heavy solid line and circles), 10.1 (squares), 10.2 (downward-pointing triangles), and 10.3 (upward-pointing triangles). The band structures for $n+\delta n$ electrons were calculated within the self-consistent virtual crystal approximation. Values of $\Delta E^{n+\delta n}(n+\delta n)$ are denoted by solid symbols. All values denoted by symbols were calculated using the iterative refinement scheme and the solid lines joining the symbols are only a guide to the eye. The calculations were performed with the experimental lattice constant for Ni in the fcc structure. The experimental value for Ni is shown as a horizontal dashed line.

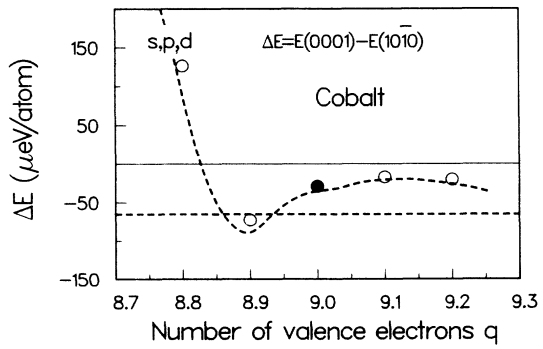

FIG. 13. $\Delta E^{n+\delta n}(n+\delta n)$ calculated with an *spd* basis in the virtual crystal approximation for $n+\delta n=8.8$, 8.9, 9.0, 9.1, and 9.2 (circles). All values were calculated using the iterative refinement scheme. The dashed line denotes $\Delta E^n(q)$ for $n=9$ as in Fig. 3. The experimental value for Co is shown as a horizontal dashed line.

not found experimental evidence in support of this feature. Part of the reason for this is that when Co is alloyed with even very small amounts of Fe ($\sim 1\%$) in order to reduce the average number of valence electrons, it undergoes a structural phase transition.[48]

C. Magnitude of the spin-orbit interaction

For a partial wave $\phi_l^\sigma(\varepsilon,r)$ with energy ε, the spin-orbit coupling parameter $\xi_l^\sigma(\varepsilon)=\int \phi_l^{\sigma 2}(\varepsilon,r)\xi(r)r^2dr$, where $\xi(r)$ is given by (6). In evaluating the integral, we have checked that it does not make any difference whether we use the minority- or majority-spin potential or their average (see Secs. II A and II D). The spin-orbit coupling parameters calculated for the d partial waves with energies corresponding to the centers,[29,30] $C_{d\sigma}$, of the majority and minority d bands are given in Table III for Fe, Co, and Ni. Because of the renormalization of the $3d$ wave function in the solid, they are about 10% larger than the values of 55, 70, and 88 meV calculated for the $d^{n-1}s^1$ configurations of free Fe, Co, and Ni atoms, respectively. The increase in $\xi_d^\sigma(C_{d\sigma})$ going from Fe$\rightarrow$Co$\rightarrow$Ni is roughly proportional[30,38] to Z^2, where Z is the atomic number.

The spin-orbit coupling parameters evaluated at the Fermi energy, $\xi_d^\uparrow(\varepsilon_F)$ and $\xi_d^\downarrow(\varepsilon_F)$, are also given in Table III. Because the partial wave $\phi_l^\sigma(\varepsilon,r)$ is normalized to unity within the atomic Wigner-Seitz sphere, bonding states with a large amplitude at the sphere boundary ($r=S$) have a correspondingly smaller amplitude at the nucleus. For antibonding states, the situation is reversed. The magnitude of the relativistic effects increases from the bottom to the top of the band, and for the transition-metal d bands this increase is by almost a factor of 2.[30,38] The minority electrons at the Fermi energy are more bonding in character than the majority electrons, so that $\xi_d^\downarrow(\varepsilon_F)<\xi_d^\uparrow(\varepsilon_F)$. As a result of the increasing exchange-splitting, whereby the potential seen by the majority d electrons is deeper than that seen by the minority d electrons, the difference between $\xi_d^\uparrow(\varepsilon_F)$ and $\xi_d^\downarrow(\varepsilon_F)$ increases on going from Ni$\rightarrow$Co$\rightarrow$Fe and is almost 30% for Fe.

Our results for ΔE with spin-orbit coupling which is 90, 100, and 110% of the *ab initio* calculated value (Table IV) indicate that for Ni and Co, respectively, roughly fourth- and second-order power laws are followed. The accuracy of the calculated MAE's does not allow a determination of the exponent to better than ± 0.5. We have encountered cases where Fermi surface effects dominate ΔE (and not just *changes* in ΔE) and lead to different dependences on ξ than ξ^4 for cubic and ξ^2 for uniaxial lattices, respectively. These results show that a small uncertainty in the value used for the spin-orbit coupling cannot account for the discrepancy between ΔE and the experimental MAE.

TABLE III. Calculated spin-orbit coupling parameters (in meV) for the majority ($\uparrow$) and minority ($\downarrow$) d partial waves at the center of the unhybridized d band, $C_{d\sigma}$, and at the Fermi energy, for Fe, Co, and Ni.

	$\xi_d^\uparrow(C_{d\uparrow})$	$\xi_d^\downarrow(C_{d\downarrow})$	$\xi_d^\uparrow(\varepsilon_F)$	$\xi_d^\downarrow(\varepsilon_F)$
Iron	62	59	69	54
Cobalt	78	76	92	79
Nickel	95	94	111	105

TABLE IV. Magnetocrystalline anisotropy energy, ΔE, in μeV/atom for different values, λ, of the strength of the spin-orbit interaction, $\lambda\xi(r)$. ΔE was calculated at the experimental volume with $l_{\max}=2$.

λ	Co $E_{0001}-E_{10\bar{1}0}$	Ni $E_{001}-E_{111}$
0.9	−25	−0.4
1.0	−29	−0.6
1.1	−35	−0.8
expt.	−65	2.7

D. Exchange-correlation potential

All the calculations mentioned so far were carried out using the parametrization of von Barth and Hedin for the exchange-correlation potential.[27] Because of the sensitivity of ΔE to the details of the band structure at ε_F, we investigated the influence of the choice of exchange-correlation potential on the anisotropy energy. Using the exchange-correlation potential of Ceperly and Alder, as parametrized by either Perdew and Zunger or by Vosko, Wilk, and Nusair,[27] we found a change in ΔE of less than 3 μeV/atom for cobalt. A large change is indeed not expected if the bands at the Fermi level do not change significantly. This is because the remainder of the anisotropy energy can be understood by means of perturbation theory on the energy bands. The ΔE which results from averaging over bands and $\mathbf{k}$ points is not sensitive to changes in the location of the energy bands of the order of 10 meV.

E. Influence of strain

All the calculations which we have discussed so far were performed using the experimental lattice parameters. It is well known that the LDA underestimates the equilibrium lattice constants of transition metals by as much as 3%.[56] Since it is not *a priori* clear whether one should compare experimental quantities with the corresponding quantities calculated at theoretical or experimental volumes, we also investigated the effect of strain on ΔE. For each value of the strain we performed a self-consistent spin-polarized band-structure calculation and evaluated ΔE by means of the force theorem. The results are given in Table V for Ni and Co. It can be seen immediately that using the theoretical volume does not lead to a value for ΔE which is in better agreement with experiment than the values calculated using the experimental volumes. We conclude that this is not the source of the disagreement with experiment.

For Fe and Ni the strain dependence of the anisotropy energies in Table V is smaller than our estimated error bars. However, it proved to be systematic and linear for Co and Ni but not for Fe. The structure in the energy

TABLE V. Magnetocrystalline anisotropy energy, ΔE, in μeV/atom for different values of strain compared to experimental values of the MAE calculated using the experimental magnetostriction constants and elastic constants. For Ni these constants were taken from Ref. 4. For Co the values given in Ref. 58 were used. The strain components which are not given explicitly are zero. The numerical uncertainty in the absolute value of the anisotropy energy is estimated to be 0.5 μeV for Ni and Fe, and 2 μeV for Co. Anisotropy energy *differences* are more reliable than this.

$E_{001}-E_{111}$	expt.	*spdf*	*spd*	strain (%)
Nickel	2.68	−0.52	−0.56	0
	2.47		−0.61	$e_{11}=e_{22}=e_{33}=-1$
	2.26		−0.68	$e_{11}=e_{22}=e_{33}=-2$
$E_{0001}-E_{10\bar{1}0}$	expt.	*spdf*	*spd*	strain (%)
Cobalt	−65	16	−29	0
	−38	19	−19	$e_{11}=e_{22}=e_{33}=-1$
	−11		−11	$e_{11}=e_{22}=e_{33}=-2$
	−92	10	−38	$e_{11}=e_{22}=-e_{33}/2=+0.33$

bands is resolved sufficiently well with our **k** grid to be able to derive an indication of the strain dependence. The corresponding experimental values which are given in Table V were obtained by expressing the strain dependence of the anisotropy constants in terms of the magnetostriction constants and the elastic constants.[57] The change in the anisotropy constants upon straining, $\Delta K(e)$, can be deduced to be

$$\Delta K_1(e)=-9h_3Be$$

for nickel and iron where only symmetry conserving strains are considered, i.e., $e_{11}=e_{22}=e_{33}=e$ and $e_{12}=e_{23}=e_{31}=0$. For cobalt we consider $e_{11}=e_{22}$ and $e_{12}=e_{23}=e_{31}=0$ and then find

$$\Delta K_{u1}(e_{11},e_{33})=-\{[(\lambda_A+\lambda_B)(C_{11}+C_{12})+2\lambda_c C_{13}]e_{11}+[(\lambda_A+\lambda_B)C_{13}+C_{33}\lambda_C]e_{33}\}\ .$$

Here, $\lambda_{A,B,C}$ and h_3 are magnetostriction constants[3,4,58] and B is the bulk modulus $(C_{11}+2C_{12})/3$. C_{ij} are elastic constants and e_{ij} are components of the strain tensor. From Table V it can be seen that the sign of the change in the anisotropy energy on straining the lattice is given correctly but the strain dependence is much smaller (a factor 5) than what is found experimentally.

V. DISCUSSION

We have seen that there is considerable disagreement between our first-order estimate ΔE for the anisotropy energy and experiment; the easy axes are predicted incorrectly for Ni and Co. Since the energies are so small, it is natural to ask how the results of the calculation depend on the various other approximations made, before attributing the failure to the LSDA. We have demonstrated that the sensitivity of the results to strain, choice of exchange-correlation potential, the magnitude of the spin-orbit coupling interaction, and to small changes in the position of the Fermi level (both within a rigid band model and within the virtual crystal approximation) is insufficient to account for the discrepancies which we have found. There are several other approximations whose effect we must consider.

Foremost among these is the approximation of the anisotropy energy by the difference in the sum of single-particle eigenvalues. In Sec. II B we showed by solving (1) self-consistently that for a particular choice of the magnetization direction the second-order change in the total energy can be substantial compared to the MAE. We could only argue that it is plausible that a systematic cancelation of the second-order corrections for two different magnetization directions will also occur. In order to show that this is so would require a computational effort which is much greater than that which is required to calculate the difference in the sum of the single-particle eigenvalues. To converge these sums reasonably well already stretches the capacity of present-day computers and we have made no attempt to go beyond the first-order approximation to the MAE. We are not aware of any attempts by others to do so. We believe that this is the largest source of uncertainty in our examination of the LSDA prediction for the MAE.

The second point which we must consider is the neglect of nonspherical terms in the potential. This can influence the value we obtain for the anisotropy energy in two ways. First, the position and dispersion of the energy bands (in the absence of spin-orbit coupling) will be modified. For states whose occupation does not change, we do not expect this effect to be important. However, if there are degenerate states close to the Fermi level whose occupation is modified, significant changes in the anisotropy energy could occur which are difficult to predict. In Co, we first identified those bands near the Fermi level whose contribution to the anisotropy energy changes substantially when their occupation is altered. We then compared those bands as calculated with (FLAPW) and without (LMTO-ASA) nonspherical contributions to the potential. The shift of these bands (17 and 18) was much smaller than what is required to bring the calculated anisotropy energy into agreement with experiment. Secondly, the spin-orbit interaction could, in principle, be modified by the nonspherical terms in the potential so that it no longer has a simple $\boldsymbol{l}\cdot\boldsymbol{\sigma}$ dependence. Because by far the major contribution to the spin-orbit coupling comes from the core region where the potential varies rapidly and where nonspherical corrections are small, we

do not expect this effect to be significant. This is confirmed by our finding that a 10% change in the strength of the spin-orbit interaction leads to changes in the calculated anisotropy energy which are not nearly enough to bring it into agreement with experiment. It seems unlikely that the nonspherical terms in the charge density will remove much of the discrepancy between ΔE and the experimental MAE.

In our calculations we have approximated the Dirac equation by the Pauli equation. The neglected terms in the Schrödinger equation are all 3 orders of magnitude smaller than the spin-orbit coupling term. There have been attempts to improve upon this treatment by solving the radial Dirac equations including a spin-dependent potential.[59] Even for a central potential the even and odd radial solutions of this Dirac equation are all coupled and only an approximate solution is possible. In tests for Ni, Ebert found essentially no difference between the results of the improved scheme and the perturbative scheme outlined in Sec. II A.[36] However, problems may certainly arise in applications of the perturbative scheme to heavier elements where the spin-orbit coupling may no longer be considered small. For example, the spin-orbit splitting of the partially occupied $5f$ states in actinide compounds is comparable to their exchange splitting and dispersion.[49]

The effects of exchange and correlation in the local-density approximation are obtained from parametrizations of the results of calculations performed for the interacting homogeneous electron gas. By considering a spin-polarized electron gas, spin-dependent exchange-correlation energies and potentials have been derived[27] and these are found to describe the ground-state properties of $3d$ transition-metal magnets reasonably well.[23] The $5f$ electrons of the actinide elements are intermediate between the $3d$ electrons of the first row transition-metal elements and the $4f$ electrons of the rare earths in terms of their localization. When the LSDA is applied to the actinide systems mentioned above, serious discrepancies with experiment are found.[60] Inclusion of relativistic effects (mass-velocity and Darwin shifts as well as spin-orbit coupling) leads to significant improvements including the prediction of large orbital magnetic moments.[32,60,61] Further improvements have been obtained by introducing a dependence of the exchange-correlation potential on the orbital angular momentum.[60,61]

On the basis of his inability to obtain realistic values for the MAE for Fe from a simple model, Jansen has concluded that a dependence of the exchange-correlation potential on the orbital angular momentum was necessary in order to calculate the magnetic anisotropy of $3d$ transition-metal elements.[62] Although we do not disagree with this conclusion, we do not believe that it may be drawn on the basis of the calculations which he presented. We have seen in Figs. 2–4, 12, and 13 that values of the MAE obtained with a realistic model (LSDA band structure including relativistic effects) have the correct order of magnitude compared with experiment. That the correct values of $\Delta E^n(n)$ are not predicted may be attributed to relatively small errors in the description of the electronic band structure. We ascribe the 2-orders-of-magnitude discrepancy for the MAE found by Jansen to his use of an oversimplified model.[62]

A. Comparison with previous work

There have been few attempts to calculate the MAE of Fe, Co, or Ni from first principles.[15–17] The calculations by Fritsche *et al.* yield an easy axis for nickel which is in agreement with experiment.[15] Their calculated value of 10 μeV is almost a factor of 4 larger than the experimental value of 2.7 μeV. In the case of iron the incorrect easy axis is predicted. The procedure adopted by Fritsche *et al.* is in many respects similar to our own. They use an atomic-sphere approximation for the crystal potential and they also use the variationality of the energy to express total-energy differences as differences in sums of single-particle eigenvalues (albeit not within the Hohenberg-Kohn-Sham framework). The principal difference between the two calculations is that these authors do not use one of the standard LSDA potentials.[27] This has as a consequence that their calculated spin moment for Ni is 10% smaller than our own (Table I). In their Brillouin-zone integral Fritsche *et al.* use a maximum sampling of $\sim(30)^3$ **k** points in the full zone compared to our maximum sampling of $(160)^3$ **k** points. Although it is impossible to say for sure what the origin is of the difference between their results and ours, we believe that a large part of it can be explained by their using a coarse BZ sampling which is far from what is necessary to obtain convergence (Figs. 5 and 7). Because no details are given as to how the BZ integral was performed, it is not clear whether or not they incur another large error because of the misweighting problem discussed in Secs. II C and III A.[42] For Fe, Fritsche *et al.* calculate the MAE to be 7.4 μeV compared to the experimental value of -1.3 μeV. A coarse BZ sampling was also used in this calculation.

More recently, Strange *et al.* have also reported a calculation of the MAE for Ni where the correct easy axis was found, albeit with a large uncertainty in the numerical value.[17] Their calculation was based on the KKR method, which assumes a spherically symmetrical potential around the atoms. The exchange splitting was treated on the same footing as the spin-orbit coupling which is, in principle, a procedure superior to ours. However, as noted by Ebert in his comparison of the two methods,[36] it leads in practice to no significant difference in the energy band dispersion and certainly none which in our experience would account for the discrepancy between their result and our own. These authors also approximated the MAE as the difference in sums of single-particle eigenvalues but unfortunately they do not give sufficient details about their k-space integration to enable us to evaluate it. [Assuming that they use 250 sampling points along each ray in their prism integration method,[59] then we estimate that they have a maximum sampling of $\sim(76)^3$ points—more than a factor 8 smaller than our maximum sampling. In addition, they do not seem to be aware of the problem of misweighting when using IBZ's (Ref. 42).] Other differences between their calculation and those presented in this publication are that they use a

complex contour integration method to simplify the BZ integration. In our experience with complex contour integration schemes this will not make the integration much simpler because in order to close the contour at the Fermi energy a very dense sampling of points about the Fermi surface is required in order to reduce the broadening of the eigenvalue spectrum.[63,64]

Similar reservations must be expressed about a calculation of the MAE as a function of c/a for Fe on a simple tetragonal lattice by the same authors.[65] Results were presented for the MAE for a very large range of axial ratios, $1.10 \leq c/a \leq 1.35$. These results were based on a potential calculated for bcc Fe in the absence of spin-orbit coupling. It is very doubtful whether this potential may be transferred to the open simple tetragonal structure for the large values of c/a examined. Because a self-consistent calculation was not performed for each value of c/a, it follows from the discussion of the force theorem in Sec. II B that an error proportional to $\Delta\rho$ [Eq. (13)] is incurred in such a procedure. In our own calculations for Co we found a difference of 100% in the change of MAE between zero and -1% strain depending on whether the zero-strain potential was used for the -1% MAE calculation or whether a self-consistent calculation was performed for -1% strain.

Calculations have recently been performed for free-standing monolayers of $3d$ transition-metal elements.[18,19] These serve as a model for overlayers of $3d$ transition metals on Cu, Ag, or Au substrates which are therefore assumed not to affect the anisotropy energy. The MAE was found to be much larger for the free-standing two-dimensional monolayers than for the three-dimensional crystals discussed so far and it was possible to obtain reasonable convergence of the (two-dimensional) reciprocal space sums. Unfortunately the two calculations cited obtain different signs for the MAE and thus predict different easy axes. A comparison of these calculations with experiment is difficult because the importance of the interaction with the substrate is not known *a priori*. By performing calculations of the MAE for monolayers of Fe on Ag substrates, it was shown that the interaction of the overlayer with the substrate cannot be assumed to be negligible and that indeed the prediction of an out-of-plane easy axis for a free monolayer of Fe was reversed on introducing the substrate.[20] Because mass-velocity and Darwin shifts, which are known to be important for Ag, were neglected in this calculation, it remains unclear what the final LSDA prediction is.

In the only other *ab initio* work on MAE we are aware of, Brooks *et al.*[49] have calculated the MAE for uranium sulphide, a compound with a NaCl structure which is ferromagnetic with a Curie temperature of 180 K. Experimentally it is known that the easy axis is in the (111) direction and the anisotropy energy has been estimated to be between 7 and 70 meV/formula unit.[66] By iterating the Hamiltonian (1) to self-consistency, Brooks *et al.* found a MAE of 204 meV/formula unit and predicted the (111) direction correctly as the easy axis.[49] Using the force theorem (14), they found a value of $\Delta E = 182$ meV/formula unit. The large value for ΔE has been attributed to the large spin-orbit splitting of the uranium $5f$ states of ~ 1 eV.

So far in this work we have been concerned with evaluating the possibility of calculating MAE's *ab initio*. It should perhaps not be surprising that the LSDA fails to yield total-energy differences correctly at the 0.1-meV level. Although we have not discussed in any detail empirical schemes where the band structure is derived by fitting to experiment,[11] one of the reasons for our attempting to calculate energy differences at the level of μeV was the remarkable success of empirical methods, in particular the work of Mori *et al.*, in reproducing the experimental MAE's. This work,[13] which is based on tight-binding band structures, supersedes the earlier extensions[7-10,12] of Brook's model[6] by using a realistic band structure and performing the necessary integrals numerically. Essentially perfect agreement with experiment is achieved. In order to perform the BZ integral Mori found that for sampling densities between $(58)^3$ and $(78)^3$ points in the full BZ there was no significant change in the calculated anisotropy constants ($< 10\%$ for K_1).[13] This is in contrast with our experience, where we find large fluctuations in the MAE for different BZ sampling densities in this range (Figs. 5 and 7). The Gilat-Raubenheimer integration method used by Mori *et al.* makes the same basic approximation of linearly interpolating the energy bands between sampling points as does the linear analytic tetrahedron method used by us. The tetrahedron method has the advantage of providing analytical expressions for the total energy, thus eliminating the energy mesh step, $d\varepsilon$, as a convergence parameter.[41] It is not clear in Mori's later work whether or not an *sp*-like band is included in the band structure. Omission of this band may possibly make the numerical convergence of the BZ integrals simpler by reducing the considerable number of band crossings in the neighborhood of the Fermi energy (Fig. 6). It is also unclear whether or not the differences in the number of electrons for the two field directions for a fixed Fermi energy, the so-called "feeble differences," are used as a disposable parameter in order to fit the calculated MAE to experiment.[13] The authors note that unless they introduce these feeble differences, they cannot obtain agreement with experiment.

Finally we consider whether bands parametrized so as to give a good fit to experimental Fermi surfaces will give a better prediction of the anisotropy energy than *ab initio* bands. Related to this is the question whether the difference between the LSDA Fermi surfaces and the experimental Fermi surfaces is the origin of the discrepancy in the results. For Ni, an indication that this is indeed the case is found in the work of Kondorskii *et al.*, who have calculated the MAE using a band structure constructed so as to reproduce the most important features of the experimental Fermi surface.[11] In particular, the X_2-hole pocket was eliminated in the parametrized band structure. These authors have made a detailed study of the local contributions to the anisotropy taking account of the deformation of the Fermi surface which was shown to constitute a significant portion of the anisotropy energy.[11] The calculated anisotropy energy is approximately a factor of 2 smaller than experiment but the correct easy

axis was obtained. Unfortunately recent work demonstrating that the density-functional Fermi surface need not necessarily coincide with the real Fermi surface calls this approach into question.[54]

VI. CONCLUSIONS

Before attempting to perform *ab initio* calculations of the MAE for systems which are not well characterized experimentally,[1,2] it is necessary to assess such schemes by using them to study systems for which there is a concensus about the experimental results. We have done this by calculating the MAE for crystalline Fe, Co, and Ni within the LSDA, the only method available at present for performing such first-principles calculations. Our numerical values for the anisotropy energy do not agree with the experimental results. We find that the MAE depends in a complicated manner on the shape of the Fermi surface, where a small number of electrons may make a sizeable contribution. The large cancelation of contributions from different parts of the Brillouin zone and the importance of the Fermi-level shifts for different magnetization directions make an estimate of the MAE without a detailed calculation very difficult. This had been found in the earlier work of Kondorskii on Ni.[11] The anisotropy energy as calculated via the Brillouin-zone sum of single-particle eigenvalues is a delicate balance between competing contributions and the integral must be performed with great care.[67] Since other LSDA calculations have restricted the calculation of the MAE to the difference in sums of single-particle eigenvalues (the force theorem), only the difference in the band structure and the handling of the Brillouin-zone integral can explain the different results which have been reported. We believe that in other studies of the MAE for Ni, convergence of this sum was not achieved[15,17] and that our results are the best approximation so far to the full LSDA result. There is still room for improvement. By performing the Brillouin-zone integral with sufficient numerical accuracy, we are able to exclude this factor as the origin of the discrepancy of our results with experiment. We identify the second-order corrections to the total energy as the most pressing issue to be addressed and not the inclusion of nonspherical corrections to the potential used to generate the band structure. To perform a calculation of the total energy including electrostatic and exchange-correlation contributions at the μeV level will not be simple. In order to do so the single-particle eigenvalue sum will have to be calculated to a comparable accuracy and we have demonstrated how difficult this is.

In summary, we conclude that it is not possible at present to calculate the MAE from first principles reliably at the 0.1-meV level. In preliminary studies of several ferromagnetic compounds where the anisotropy energy is larger (MnAs, MnSb, and YCo_5) we still find quantitative discrepancies with experiment when we use the same approximations as we have used in this publication. However, the easy axes appear to be predicted correctly.[64]

ACKNOWLEDGMENTS

We wish to thank Prof. Dr. H.J.F. Jansen for stimulating and helpful discussions.

[1]C. Liu, E. R. Moog, and S. D. Bader, Phys. Rev. Lett. **60**, 2422 (1988); D. Pescia *et al.*, *ibid.* **58**, 2126 (1987).

[2]P. F. Carcia, A. D. Meinholdt, and A. Suna, Appl. Phys. Lett. **47**, 178 (1985); H. J. G. Draaisma, W. J. M. de Jonge, and F. J. A. den Broeder, J. Magn. Magn. Mater. **66**, 351 (1987); F. J. A. den Broeder, D. Kuiper, H. C. Donkersloot, and W. Hoving, Appl. Phys. A **49**, 507 (1989).

[3]D. M. Paige, B. Szpunar, and B. K. Tanner, J. Magn. Magn. Mater. **44**, 239 (1984).

[4]J. J. M. Franse, Ph.D. thesis, University of Amsterdam, 1969 (unpublished); P. Escudier, Ann. Phys. **9**, 125 (1975).

[5]J. H. van Vleck, Phys. Rev. **52**, 1178 (1937).

[6]H. Brooks, Phys. Rev. **58**, 909 (1940).

[7]G. C. Fletcher, Proc. R. Soc. London **67A**, 505 (1954).

[8]J. C. Sloncewskij, J. Phys. Soc. Jpn. **17**, Suppl. B-1, 34 (1962).

[9]W. N. Furey, Ph.D. thesis, Harvard University, 1967 (unpublished).

[10]M. Asdente and M. Delitala, Phys. Rev. **163**, 497 (1967).

[11]E. I. Kondorskii and E. Straube, Pis'ma Zh. Eksp. Teor. Fiz. **63**, 356 (1972) [JETP Lett. **36**, 188 (1973)]; E. I. Kondorskii, IEEE Trans. Mag. **10**, 132 (1974).

[12]N. Mori, J. Phys. Soc. Jpn. **27**, 307 (1969); N. Mori, Y. Fukuda, and T. Ukai, *ibid.* **37**, 1263 (1974); N. Mori, T. Ukai, and H. Yoshida, *ibid.* **37**, 1272 (1974).

[13]N. Mori, T. Ukai, and S. Ohtsuka, J. Magn. Magn. Mater. **31-34**, 43 (1983); T. Tatebayashi, S. Ohtsuka, T. Ukai, and N. Mori, *ibid.* **54-57**, 973 (1986).

[14]A. J. Bennett and B. R. Cooper, Phys. Rev. B **3**, 1642 (1971); H. Takeyama, K. P. Bohnen, and P. Fulde, *ibid.* **14**, 2287 (1976); P. Bruno, J. Phys. F **18**, 1291 (1988); P. Bruno and J. Seiden, J. Phys. (Paris) Colloq. **49**, C8-1645 (1988).

[15]L. Fritsche, J. Noffke, and H. Eckardt, J. Phys. F **17**, 943 (1987).

[16]G. H. O. Daalderop, P. J. Kelly, M. F. H. Schuurmans, and H. J. F. Jansen, J. Phys. (Paris) Colloq. **49**, C8-93 (1988).

[17]P. Strange, H. Ebert, J. B. Staunton, and B. L. Gyorffy, J. Phys. Condens. Matter **1**, 3947 (1989).

[18]J. G. Gay and R. Richter, Phys. Rev. Lett. **56**, 2728 (1986).

[19]W. Karas, J. Noffke, and L. Fritsche, J. Chim. Phys. Phys.-Chim. Biol. **86**, 861 (1989).

[20]J. G. Gay and R. Richter, J. Appl. Phys. **61**, 3362 (1987).

[21]P. Hohenberg and W. Kohn, Phys. Rev. **136**, B864 (1964).

[22]W. Kohn and L. J. Sham, Phys. Rev. **140**, A1133 (1965).

[23]See the collection of articles in *Theory of the Inhomogeneous Electron Gas,* edited by S. Lundqvist and N. H. March (Plenum, New York, 1983).

[24]O. Gunnarsson and R. O. Jones, Rev. Mod. Phys. **61**, 689 (1989).

[25]The generalization of spin-density-functional theory within a fully relativistic framework is discussed by A. K. Rajagopal and J. Callaway, Phys. Rev. B **7**, 1912 (1973); A. H. MacDonald and S. H. Vosko, J. Phys. C **12**, 2977 (1979); H. Eschrig, G. Seifert, and P. Ziesche, Solid State Commun. **56**, 777 (1985).

[26]For a discussion of the application of relativistic density-functional theory to magnetocrystalline anisotropy, see H. J. F. Jansen, Phys. Rev. B **38**, 8022 (1988).

[27]U. von Barth and L. Hedin, J. Phys. C **5**, 1629 (1972); O. Gunnarsson and B. I. Lundqvist, Phys. Rev. B **13**, 4274 (1976); S. H. Vosko, L. Wilk, and M. Nusair, Can. J. Phys. **58**, 1200 (1980); J. P. Perdew and A. Zunger, Phys. Rev. B **23**, 5048 (1981).

[28]C. S. Wang, B. M. Klein, and H. Krakauer, Phys. Rev. Lett. **54**, 1852 (1985); K. B. Hathaway, H. J. F. Jansen, and A. J. Freeman, Phys. Rev. B **31**, 7603 (1985); H. J. F. Jansen, K. B. Hathaway, and A. J. Freeman, *ibid.* **30**, 6177 (1984); H. J. F. Jansen and S. S. Peng, *ibid.* **37**, 2689 (1988).

[29]O. K. Andersen, Phys. Rev. B **12**, 3060 (1975).

[30]O. K. Andersen, O. Jepsen, and D. Glötzel, in *Highlights in Condensed Matter Theory,* edited by F. Bassani, F. Fumi, and M. P. Tosi (North-Holland, Amsterdam, 1985), p. 59.

[31]M. Singh, J. Callaway, and C. S. Wang, Phys. Rev. B **14**, 1214 (1976).

[32]M. S. S. Brooks and P. J. Kelly, Phys. Rev. Lett. **51**, 1708 (1983).

[33]O. Gunnarsson, Physica B+C (Amsterdam) **91B**, 329 (1977); J. F. Janak, Phys. Rev. B **16**, 255 (1977).

[34]O. K. Andersen, J. Madsen, U. K. Poulsen, O. Jepsen, and J. Kollar, Physica B+C (Amsterdam) **86-88B**, 249 (1977).

[35]D. D. Koelling and B. N. Harmon, J. Phys. C **10**, 3107 (1977); H. Gollisch and L. Fritsche, Phys. Status Solidi B **86**, 145 (1978); J. H. Wood and A. M. Boring, Phys. Rev. B **18**, 2701 (1978).

[36]H. Ebert, Phys. Rev. B **38**, 9391 (1988).

[37]O. Gunnarsson, J. Harris, and R. O. Jones, Phys. Rev. B **15**, 3027 (1977).

[38]A. R. Mackintosh and O. K. Andersen, in *Electrons at the Fermi Surface,* edited by M. Springford (Cambridge University Press, Cambridge, 1980); M. Weinert, R. E. Watson, and J. W. Davenport, Phys. Rev. B **32**, 2115 (1985).

[39]The energy shift in second-order perturbation theory is given by

$$\Delta E_2 = -\sum_{\mathbf{k}} \sum_{n}^{\text{occ}} \sum_{m}^{\text{unocc}} \frac{|\langle m,\mathbf{k}|\xi \boldsymbol{l}\cdot\mathbf{s}|n,\mathbf{k}\rangle|^2}{\varepsilon_m(\mathbf{k})-\varepsilon_n(\mathbf{k})} .$$

When $|\varepsilon_m(\mathbf{k})-\varepsilon_n(\mathbf{k})| \sim \xi$ degenerate perturbation theory should be used. The occupation of states close to the Fermi level may change as a result of the perturbation and this should be taken into account when calculating magnetocrystalline anisotropy energies.

[40]O. Jepsen and O. K. Andersen, Solid State Commun. **9**, 1763 (1971); G. Lehmann and M. Taut, Phys. Status Solidi B **54**, 469 (1972).

[41]See Refs. 13 and 19.

[42]L. Kleinman, Phys. Rev. B **28**, 1139 (1983); O. Jepsen and O. K. Andersen, *ibid.* **29**, 5965 (1984).

[43]O. K. Andersen, P. Blöchl, and O. Jepsen, Bull. Am. Phys. Soc. **33**, 804 (1988); P. Blöchl, Ph.D. thesis, University of Stuttgart, 1989 (unpublished).

[44]H. J. F. Jansen and A. J. Freeman, Phys. Rev. B **30**, 561 (1984).

[45]O. K. Andersen and O. Jepsen, Phys. Rev. Lett. **53**, 2571 (1984).

[46]B. R. A. Nijboer and F. W. De Wette, Physica (Amsterdam) **23**, 309 (1957); F. S. Ham and B. Segall, Phys. Rev. B **124**, 1786 (1961).

[47]B. R. A. Nijboer and F. W. De Wette, Physica (Amsterdam) **24**, 422 (1958).

[48]*Landolt-Börnstein, New Series,* Vol. III/19a, edited by H. P. J. Wein (Springer, Berlin 1988).

[49]M. S. S. Brooks, B. Johansson, O. Eriksson, and H. L. Skriver, Physica B+C (Amsterdam) **144B**, 1 (1986).

[50]J. Friedel, in *The Physics of Metals,* edited by J. M. Ziman (Cambridge University Press, Cambridge, 1969).

[51]A. V. Gold, J. Low-Temp. Phys. **16**, 3 (1974).

[52]C. S. Wang and J. Callaway, Phys. Rev. B **9**, 4897 (1974); E. I. Zornberg, *ibid.* **1**, 244 (1970).

[53]R. Gersdorf, Phys. Rev. Lett. **40**, 344 (1978).

[54]K. Schönhammer and O. Gunnarsson, Phys. Rev. B **37**, 3128 (1988); D. Mearns, *ibid.* **38**, 5906 (1988).

[55]This result has been derived for the high-symmetry lines R, S, and S' when the external field is aligned along high-symmetry directions by A. P. Cracknell, J. Phys. C **2**, 1425 (1969); Phys. Rev. B **1**, 1261 (1970).

[56]For results of LSDA calculations where shape approximations to the potential (muffin-tin, atomic sphere) have been made, see V. Moruzzi, J. Janak, and A. R. Williams, *Calculated Electronic Properties of Metals* (Pergamon, New York, 1978); O. K. Andersen, O. Jepsen, and D. Glötzel (Ref. 30). There have been several calculations for Fe without any shape approximation (Ref. 28). For Co extensive calculations with the FLAPW method have been performed (G. H. O. Daalderop and H. J. F. Jansen, unpublished).

[57]R. R. Birss, *Symmetry and Magnetism* (North-Holland, Amsterdam, 1964). The case of cubic symmetry has been discussed by Franse (Ref. 4). The hcp case has been discussed by M. S. S. Brooks and D. A. Goodings, J. Phys. C **1**, 1279 (1968).

[58]A. Hubert, W. Unger, and J. Kranz, Z. Phys. **224**, 148 (1969).

[59]R. Feder, F. Rosicki, and B. Ackermann, Z. Phys. B **52**, 31 (1983); P. Strange, J. B. Staunton, and B. L. Gyorffy, J. Phys. C **17**, 3355 (1984); P. Strange, H. Ebert, J. B. Staunton, and B. L. Gyorffy, J. Phys. Condens. Matter **1**, 2959 (1989).

[60]M. S. S. Brooks, Physica B+C (Amsterdam) **130B**, 6 (1985).

[61]O. Eriksson, M. S. S. Brooks, and B. Johansson, Phys. Rev. B (to be published). O. Eriksson, Ph.D. thesis, University of Uppsala, 1989 (unpublished).

[62]H. J. F. Jansen, J. Appl. Phys. **64**, 5604 (1988).

[63]A. R. Williams, P. J. Feibelman, and N. D. Lang, Phys. Rev. B **26**, 5433 (1982).

[64]G. H. O. Daalderop, P. J. Kelly, and M. F. H. Schuurmans, unpublished.

[65]P. Strange, J. B. Staunton, and H. Ebert, Europhys. Lett. **9**, 169 (1989).

[66]D. L. Tillwick and P. de V. du Plessis, J. Magn. Magn. Mater. **3**, 329 (1976); G. H. Lander, M. S. S. Brooks, B. Lebech, P. J. Brown, and O. Vogt, unpublished.

[67]After this work was completed we implemented the scheme proposed by Blöchl *et al.* (Ref. 43) to take account, approximately, of the curvature of the filled bands in the BZ sum of the single-particle eigenvalues. In those cases (e.g., Co, Fig. 8) where the anisotropy energy follows a $v^{2/3}$ behavior, Blöchl's procedure yields essentially the same result as the value obtained by extrapolating ΔE to zero volume (Fig. 8). This indicates that the curvature of the bands at the Fermi energy, which is taken into account by our extrapolation but not in Blöchl's approximation, is not significant. For Ni, where extrapolation of ΔE proportional to $v^{2/3}$ to $v \rightarrow 0$ may only be carried out when the mesh is sufficiently dense that all important band crossings are resolved (Figs. 5 and 6), Blöchl's procedure also fails to yield any improvement.